The Effects of Whole-Body Heating on Serotonergic Systems: A Novel Mechanism for Treating Depression

Alexander S. Jones

Department of Integrative Physiology

University of Colorado Boulder

Defended April 3rd, 2015

Thesis Advisor:
Dr. Christopher A. Lowry, Department of Integrative Physiology and the Center for Neuroscience

Defense Committee:
Dr. David Sherwood, Department of Integrative Physiology
Dr. Rebecca Ciancanelli, Student Academic Success Center

Table of Contents

Abstract

Major depressive disorder (MDD) is projected to be the 2nd leading cause of disability-adjusted life years (DALYs) by 2020. One hypothesis is that dysfunction of serotonergic systems in the brain, particularly serotonergic systems in the dorsal raphe nucleus, plays a role in the etiology and pathophysiology of depression. Current antidepressant therapies include drug therapies such as selective serotonin reuptake inhibitors (SSRIs). Although SSRIs have antidepressant effects in severely depressed patients, they also have many deleterious side effects. Thus, there is a need for more effective treatments that have fewer negative side effects. To develop more effective treatments for depression, a greater understanding of the underlying physiological mechanisms involved in activation of brainstem serotonergic systems and antidepressant responses is needed. Previous studies have demonstrated that whole-body heating in rats can activate a putative antidepressant-related subset of serotonergic neurons in the interfascicular part of the dorsal raphe nucleus. However, the pathway(s) involved in 1) activation of serotonergic neurons, and 2) activation of forebrain systems implicated in MDD, by warm temperature are not known. Here we explored neural systems activated by whole-body heating in rats, particularly spinoparabrachial and spinothalamic pathways, in hopes of identifying potential mechanisms through which whole-body heating activates forebrain systems implicated in antidepressant responses. We exposed rats to an incubation chamber at either warm ambient temperature (37 °C) or room temperature (RT; 23 °C) for 105 min. Brains then were removed and processed for immunohistochemical detection of the protein product of the immediate-early gene *c-fos* (as a marker of neuronal activation) and tryptophan hydroxylase (as a marker of serotonergic neurons). Our data suggest that the spinoparabrachial pathway plays a primary role in activation of brainstem serotonergic systems, while the medial spinothalamic pathway plays a direct role in activation of prefrontal cortical structures implicated in the pathophysiology of MDD and antidepressant responses. Together, these results provide evidence for multiple pathways through which warm temperature may influence affective and cognitive function, including 1) activation of prefrontal circuits via the spinoparabrachial pathway and serotonergic systems, and 2) modulation of affective and cognitive circuits via the medial spinothalamic pathway. Furthermore, these findings demonstrate the potential of whole-body heating as a novel mechanism for treating depression.

Abbreviations

AIP, agranular insular cortex; Cg1, cingulate cortex area 1; DRC, dorsal raphe nucleus, caudal part; DRD, dorsal raphe nucleus, dorsal part; DRI, dorsal raphe nucleus, interfascicular part; DRV, dorsal raphe nucleus, ventral part; DRVL, dorsal raphe nucleus, ventrolateral part; VLPAG, ventrolateral periaqueductal gray; mlf, medial longitudinal fasciculus.IL, infralimbic cortex; LPBd, lateral parabrachial nucleus, dorsal part; LPBel, lateral parabrachial nucleus, external part; MD, mediodorsal thalamic nucleus; mOFC, medial orbital cortex; MPA, medial preoptic area; NAcbSh, accumbens nucleus, shell; PrL, prelimbic cortex; PVP, paraventricular thalamic nucleus, posterior part; S1Tr, primary somatosensory cortex, trunk region; VP, ventral pallidum; VPL, ventral posterolateral thalamic nucleus; and VPM, ventral posteromedial thalamic nucleus

Introduction

Major depressive disorder (MDD) is projected to be the 2nd leading cause of disability adjusted life years (DALYs) worldwide by 2020 (Murray and Lopez, 1996). Millions of people in the United States alone will experience a depressive episode in any one year (Bromet et al, 2011). Not only is it a burden to patients suffering with MDD, but also to the economy with costs exceeding 83 billion in 2000 and increasing (for review, see Mathers and Loncar, 2006). Current treatments only help 50% of depressed patients recover in less than 12 weeks (Keller et al., 1992). Although current treatments may have some efficacy, they are also associated with many adverse side effects. Taken together, these findings indicate a need for more effective treatments with fewer adverse side effects.

To develop more effective treatments for MDD, a greater understanding of the physiology of MDD and antidepressant responses is required. Recent growth in the field of neuroscience has led to extensive research aimed at further understanding the underlying physiological mechanisms that are associated with the etiology and pathophysiology of MDD. Convergent evidence suggests that thermoregulatory systems are involved in both the etiology and pathophysiology of MDD, and also antidepressant therapeutic responses (Raison et al, 2015). Consistent with this hypothesis, infrared whole-body heating, in an open trial, had antidepressant responses that were associated with altered thermoregulatory function measured 1 week after treatment (Hanusch et al, 2013). Consequently, a better understanding of mechanisms through which whole-body heating alters neural systems, particularly those implicated in the pathophysiology of MDD, and those implicated in antidepressant responses, is desirable. Of particular interest is the dorsal raphe nucleus (DR), which may play an important role in both the pathophysiology of MDD and its treatment (Lira et al, 2003; Michelson et al, 2007; Yang et al, 2008). The DR, located on the midline of the brainstem, primarily uses the neurotransmitter serotonin, and altered serotonin levels are known to be associated with depression (for review, see Mann, 1999; Barton et al, 2008). Although the DR serotonergic system is associated with MDD and its treatment, it contains numerous anatomically distinct subpopulations of which the affective functions are not well understood. One subpopulation of the DR that has received a great deal of attention in recent studies is the interfascicular part of dorsal raphe nucleus (DRI). DRI serotonergic systems project to forebrain circuits implicated in the pathophysiology of MDD (Drevets et al, 2008; Lowry et al, 2009; Drevets and Price, 2010) and are uniquely sensitive to

environmental stimuli such as warm and cold temperature (Hale et al, 2013). Therefore, finding a novel way to properly regulate this circuit may provide a novel means of treating depression with minimal side effects.

Electrophysiological recordings done in the 1970s have found that cutaneous warming activates serotonergic neurons in the DRI region (for review, Lowry et al, 2009). Multiple studies have since supported this finding by demonstrating exposure to warm ambient temperature signals to the brain via a spinoparabrachial pathway (Nakamura & Morrison, 2009) that is thought to activate DRI serotonergic neurons (Lowry et al, 2009; Hale et al, 2011). Although the warm-sensitive nature of the DRI has been shown, the afferent mechanisms involved in activation of DRI serotonergic neurons by warm temperature have not been defined. Likewise, the afferent mechanisms involved in activation of prefrontal cortical structures implicated in affective disorders also have not been defined.

A number of studies have indicated that warm temperature exposure has multiple distinct signaling modalities, including those involved in thermoregulation, discrimination, and affect. When mammals are exposed to warm temperatures, somatosensory warm sensitive neurons are thought to relay sensory information to the brain, which results in thermoregulatory cooling (Lowry et al., 2009; Smith et al., 1998; Toth et al., 2006). Environmental increases in temperature are sensed by these somatosensory neurons which relay the thermal signal to somatosensory neurons in the dorsal horn (Lumpkin & Caterina, 2007). The neurons from the dorsal horn of the spinal cord relay numerous signals to the lateral parabrachial nucleus (LPB) (Cechetto & Staneart, 1985; Bernard et al., 1995; Feil & Herbert, 1995). Recently, it has been discovered that neurons in the LPB mediate heat loss by signaling peripheral thermoregulatory effectors (Nakamura & Morrison, 2008) through the preoptic area (POA) (Nakamura & Morrison 2009). Although the spinoparabrachial pathway may play a role in thermoregulation, the spinothalamic pathway has been indicated for its role in discrimination. Previous studies have shown that somatosensory stimuli such as warm sensations are integrated in the thalamus via the lateral spinothalamic pathway, which relays signals to the cerebral cortex (Cechetto & Saper, 1987; Craig et al, 2000; Burstein et al, 2010). Furthermore, it has been suggested that afferent signals that modulate cognitive and affective functions also follow the spinothalamic tract (McGlone et al., 2014). Clarifying the role of the spinoparabrachial and spinothalamic pathways in the effects of warm ambient temperature on affect is a question that still

remains to be teased apart.

The primary goal of this study is to further understand the role of the spinoparabrachial and spinothalamic pathways in DR activation after whole-body heating. We hypothesized that warm ambient temperature activates the spinoparabrachial pathway which serves a thermoregulatory and affective function. Furthermore, we hypothesized that warm ambient temperature activates the spinothalamic pathway which primarily serves a discriminatory function, while augmenting the affective function of the spinoparabrachial pathway. First, we implemented immunohistochemical procedures to quantify levels of activation in components of both the spinoparabrachial and spinothalamic pathways after exposure to warm ambient temperature. Second, we correlated activation of the brainstem components of the spinoparabrachial and spinothalamic pathways with activation in cortical structures that are thought to mediate discriminative and affective components of cutaneous warm temperature (Raison et al, 2015).

Materials and Methods

The tissue sampled in this study was prepared for a previous study (Hale et al, 2011), and therefore, portions of the materials and methods are taken directly from the initial study.

Animals

Adolescent male outbred Wistar rats (Hsd:WI; Harlan Laboratories, Indianapolis, IN, USA; *N* = 24) arrived from the vendor weighing 85.7 ± 7.2 g. Rats were individually housed for 10 days prior to the experiment to minimize the variability of cutaneous temperature that may be affected during nesting, grooming and play (cage dimensions, 11.5″L × 7.5″W × 5″H; bedding, 2 cm deep, Teklad Laboratory Grade Aspen Bedding, Cat No. 7088, Harlan, Madison, WI, USA). Room temperature was maintained at 22 °C. Rats were kept under a reversed 12:12 light/dark cycle with lights off at 5 AM; the light intensity during the light phase was 360 lux. Experimental procedures were performed during the dark phase. Food (Cat. No. 2018, Teklad Global 18% Protein Rodent Diet, Harlan, Madison, WI, USA) and water were available *ad libitum* for the duration of the experiment. Rats were weighed and habituated to the incubation chamber (Binder APT.Line® BD E2 Incubator with natural convection, Tuttlingen, Germany) at room temperature (23 °C) for 30 min each day prior to the test day. By the time they were tested the rats weighed 153.4 ± 11.0 g. Four rats were transferred, while they each remained in their home cages, to the incubation chamber at a time. All animal procedures were approved by the Institutional Animal Care and Use Committee (IACUC) at the University of Colorado Boulder and were conducted in accordance with the National Institutes of Health *Guide for the Care and Use of Laboratory Animals* (NIH Publications No. 80-23) revised 1996 (Institute of Laboratory Animal Resources Commission on Life Sciences National Research Council, 1996). In addition, all work was carried out in accordance with the *EC Directive 86/609/EEC for animal experiments* http://ec.europa.eu/environment/chemicals/lab_animals/legislation_en.htm and with the *Uniform Requirements for manuscripts submitted to Biomedical journals*, http://www.icmje.org.

Rectal temperature

Rectal temperature (T_{rec}; colonic, deep or core body temperature (Gordon, 1990)) was measured using a digital rectal thermometer (Ellab, Model No. DM852, Hilleroed, Denmark). Following lubrication with petroleum jelly, the temperature probe was inserted approximately 6.5 cm beyond the rectal opening for approximately 30 s until a stable temperature was reached. A single baseline temperature measurement was taken immediately before the habituation session 5 days prior to test; a second temperature measurement was taken immediately after exposure to the incubation chamber on the test day; T_{rec} was not taken immediately before exposure to the incubation chamber on the test day to eliminate the possibility of c-Fos expression due to the T_{rec} measurement procedure.

Experimental procedures

Eight rats were tested each day across 3 consecutive days, between 9 AM and 2 PM, using a single incubation chamber. The incubation chamber was set to either 37 °C or 23 °C (for room temperature (RT) controls), and individual rats were tested only once. Experimental conditions were counterbalanced within each day and across the three test days to avoid time of day or day effects. Four rats, each in a separate cage, were placed in the chamber for 105 min. Immediately following removal from the incubation chamber, T_{rec} was measured. Rats were then deeply anesthetized with sodium pentobarbital (90 mg/kg; Fatal-Plus, Vortech Pharmaceutical, Dearborn, MI, USA).

Tissue processing

Following the induction of anesthesia, rats were transcardially perfused with 0.05 M phosphate buffered saline (PBS, pH 7.4) followed by a 4% paraformaldehyde solution (prepared using 80 g paraformaldehyde, 30 g sucrose, 4.8 ml sodium hydroxide, 808 ml 0.2 M $Na_2HPO_4 \cdot 7H_20$, 192 ml $NaH_2PO_4 \cdot H_2O$, and 1 l distilled H_2O (dH_2O)). Following fixation, the brains were removed and post-fixed in the same 4% paraformaldehyde solution for 24 h at 4 °C and were then rinsed in 0.1 M sodium phosphate buffer (PB; 80.8% 0.1 M $Na_2HPO_4 \cdot 7H_2O$ and 19.2% 0.1 M $NaH_2PO_4 \cdot H_2O$) twice for 12 h each. The brains were then placed in 30% sucrose in 0.1 M PB until the brains had sunk. Brains were then blocked into forebrain and hindbrain pieces with a cut in the coronal plane at the caudal border

of the mammillary bodies (approximately −5.30 mm bregma) using a rat brain matrix (RBM-4000C, ASI Instruments, Warren, MI, USA), to ensure a consistent coronal plane of sectioning, and rapidly frozen in isopentane chilled on dry ice. The brains were then stored at −80 °C. Brain sections (30 μm) were then made using a cryostat (Leica CM1900, North Central Instruments, Denver, CO, USA) and stored as 6 alternate sets of sections. The tissue was stored at −20 °C in cryoprotectant (prepared using 270 ml ethylene glycol, 160 ml glycerol, 202 ml 0.2 M $Na_2HPO_4 \cdot 7H_2O$, 48 ml 0.2 M $NaH_2PO_4 \cdot H_2O$, and 320 ml dH_2O) until immunohistochemical procedures were conducted.

Immunohistochemistry

Tryptophan hydroxylase antibody characterization

For immunodetection of tryptophan hydroxylase (Tph), we used an affinity isolated antibody (sheep anti-TPH antiserum, Cat. No. T8575, Lot No. 096K1026 or 047K1223, Sigma-Aldrich, St. Louis, MO, USA), raised against recombinant rabbit Tph isolated as inclusion bodies from *Escherichia coli* and purified by preparative SDS-PAGE, as immunogen. To determine if this antibody has selectivity for the Tph1 or Tph2 isoform (Walther et al., 2003), dual label immunofluorescence was conducted using the Sigma-Aldrich sheep anti-Tph and monospecific polyclonal antibodies raised against either Tph1 or Tph2 peptide antigens from non-overlapping sequences in their respective proteins (for details, see Sakowski et al., 2006), which was kindly supplied by Professor Donald M. Kuhn.

Two sets of adjacent (30 μm apart) brain sections, including the DR and the pineal gland, were sampled from one rat from the RT exposed group. Tissue was washed twice for 15 min in 0.05 M PBS, then preincubated for 60 min in 0.05 M PBS with 0.1% Triton X-100 (Cat No. T9284, Batch No. 017 K00112, Sigma-Aldrich; 0.1% PBST). Brain sections were then incubated overnight at RT with either: 1) rabbit anti-Tph1 antibody (1:500) and sheep anti-Tph antibody (1:1000), or 2) rabbit anti-Tph2 antibody (1:500) and sheep anti-Tph antibody (1:1000) in 0.05 M PBS. After 16 h the tissue was washed twice for 15 min in 0.05 M PBS followed by incubation for 90 min with donkey anti-rabbit FITC (1:200; Cat. No. 711-096-152, Lot No. 81514, Jackson ImmunoResearch, West Grove, PA, USA) and donkey anti-sheep Cy5 (1:200, Cat. No. 713-176-147, Lot No. 80271, Jackson ImmunoResearch) in 0.05 M PBS. Tissue was then rinsed for 15 min in 0.05 M PBS and mounted on glass slides (VistaVision, Cat No. 16004-382,

VWR, West Chester, PA, USA) and mounted with cover slips using Vectashield mounting medium for fluorescence with DAPI (Cat. No. H-1200, Vector Laboratories). Nail polish was used to seal the outer edges of the cover slips.

Dorsal raphe nucleus

One set of midbrain sections, including the midbrain raphe complex, was used for double immunostaining using primary antibodies directed against the protein product of the immediate-early gene *c-fos* (1:3000, rabbit anti-c-Fos polyclonal antiserum, Cat. No. PC38, Lot No. D00015268, 1:3000; Calbiochem (EMD Chemicals) Gibbstown, NJ, USA), and against Tph (1:12,000, sheep anti-TPH antiserum, Cat. No. T8575, Lot No. 096K1026; Sigma-Aldrich). Tissue was washed twice in 0.05 M PBS, then rinsed in 1% H_2O_2 in 0.05 M PBS, followed by washing in 0.05 M PBS and preincubation in 0.05 M PBS with 0.3% Triton X-100 (Cat No. T9284, Batch No. 017K00112, Sigma-Aldrich; 0.3% PBST). Sections were then incubated overnight at RT with rabbit anti-c-Fos polyclonal antiserum (1:3000) in 0.05 M PBS with 0.1% Triton X-100 (0.1% PBST). After 16 h, tissue was washed twice in 0.05 M PBS followed by incubation with a biotinylated donkey anti-rabbit secondary antibody (1:200, Cat. No. E0353, Lot No. E035301028501-0802, DAKO, Carpinteria, CA, USA) in 0.05 M PBS for 90 min. Tissue was washed twice in 0.05 M PBS followed by incubation with an avidin–biotin–peroxidase complex (Elite ABC reagent, Cat. No. PK-6100, 1:200; Vector Laboratories, Burlingame, CA, USA) in 0.05 M PBS for 90 min. Tissue was then washed twice in 0.05 M PBS, and incubated in a peroxidase chromogen substrate (Vector SG; Vector Laboratories; Cat. No. SK4700; diluted as recommended by the vendor) in 0.05 M PBS for 18 min. After the chromogen reaction, tissue was immediately washed in 0.05 M PBS, then in 1% H_2O_2 in 0.05 M PBS, and twice in 0.05 M PBS. The tissue was then incubated with sheep anti-Tph antiserum (1:12,000) in 0.1% PBST overnight at RT. All subsequent steps were identical to those described earlier for the immunoperoxidase localization of c-Fos immunoreactivity, except for the secondary antibody and chromogen reaction steps; these used a rabbit anti-sheep secondary antibody (1:200, Cat. No. PK-6106, Vector Laboratories), and a peroxidase chromogen substrate solution consisting of 0.01% 3,3′-diaminobenzidine tetrahydrochloride (DAB; Cat. No. D9015, Lot No. 85897LJ, Sigma-Aldrich) and 0.0015% H_2O_2 in 0.05 M PBS (25 min). Finally, sections were washed twice in 0.05 M

PBS to stop the reaction. Brain sections were rinsed briefly in distilled water with 0.15% gelatin (gelatin from porcine skin, type A, Cat. No. G-2500, Batch No. 087K0125, Sigma-Aldrich) then mounted on microscope slides (VistaVision, VWR), dehydrated through an alcohol series and cleared with xylene. The slides were then mounted with cover slips using Entellan mounting medium (Electron Microscopy Science, Hatfield, PA, USA). The color reaction of the c-Fos immunostaining was blue–black and localized to the cell nucleus while that of the Tph immunostaining was orange–brown and localized to the cytoplasm.

Spinoparabrachial and spinothalamic systems

The procedure for immunohistochemical staining of the spinoparabrachial and spinothalamic systems was identical to that used for the DR with the exception that Tph immunostaining was not done on these sections.

Cell counting, dorsal raphe nucleus

The numbers of c-Fos-immunoreactive (c-Fos-ir) serotonergic neurons (i.e. c-Fos-ir/Tph-ir neurons), the numbers of c-Fos-ir, non-serotonergic cells (i.e. c-Fos-ir/Tph-immunonegative cells), and the total numbers of Tph-ir neurons sampled (i.e. both c-Fos-ir/Tph-ir and c-Fos-immunonegative/Tph-ir neurons) were counted in subdivisions of the DR at five rostrocaudal levels (−7.46, −8.18, −8.36, −8.54, and −8.72 mm bregma). The subdivisions and rostrocaudal levels of the DR that were sampled are illustrated in Figure 1. The boundaries for the subdivisions of the DR that were sampled were based on the anatomical location of each subdivision and the density and morphology of the serotonergic neurons within each subdivision. Briefly, the DR, dorsal part (DRD) at −7.46 mm and −8.18 mm bregma is bordered dorsally by the cerebral aqueduct, ventrally by the DR, ventral part (DRV) and laterally by the DRVL/VLPAG at −8.18 mm bregma (1A and 1B). The DRD contains mostly medium-sized, fusiform or bipolar cells oriented in the rostrocaudal direction (Steinbusch, 1984). The DRV is bordered dorsally by the DRD, ventrally and laterally by the medial longitudinal fasciculus (mlf) and decussation of the superior cerebral peduncle (xscp) except at its most caudal extent where it merges with the DRI. The DRV is characterized by densely packed serotonergic neurons, which allow it to be distinguished from the

DRD (Steinbusch, 1984). The DRVL/VLPAG region is located lateral to the DRD and DRV and consists of serotonergic neurons that are notable for their large size, relative to other subpopulations of serotonergic neurons in the DR, and their multipolar morphology (Steinbusch, 1984). The DRI consists of bilateral columns of serotonergic neurons located between the mlf (1C, 1D, and 1E). DRI serotonergic neurons are morphologically distinct from other regions of the DR in that they are spindle-shaped and oriented in a vertical plane (Azmitia and Gannon, 1986). The DR, caudal part (DRC) is the most caudal aspect of the DR and is bordered dorsally by the cerebral aqueduct and ventrally by the DRI (Figs 1C, 1D, and 1E). The DRC contains small round serotonergic neurons at its rostral extent and medium-size serotonergic neurons at its rostral and caudal extents (Steinbusch, 1984). Midline serotonergic neurons in the DRC have short thick dendrites orientated dorsoventrally, while the lateral serotonergic neurons have longer dendritic processes extending dorsolaterally along the ventral surface of the cerebral aqueduct (Hale et al., 2010). The DRVL/VLPAG at −8.18 mm bregma is a bilateral structure. Cells were counted in both the left and the right DRVL/VLPAG and the cell counts were summed to give a total number of cells in the DRVL/VLPAG. For the remaining subdivisions, which are all located on the midline, cells were counted on both the left and right sides of the midline and the cell counts were summed to give a total number of cells in each subdivision.

Round or oval-shaped cell nuclei with blue/black immunostaining darker than the background were counted as c-Fos-ir nuclei. Cells with orange/brown cytoplasmic immunostaining darker than the background were counted as Tph-ir neurons. Cells with blue/black nuclei and brown/orange cytoplasmic staining were counted as c-Fos-ir/Tph-ir (double-immunostained) neurons. One section from each rat at each anatomical level was sampled. Cell counts were conducted using a 10× objective (100× total magnification) by two investigators (KFD and MWH) blind to the assignment of treatment groups (inter-rater reliability for the complete DR data set: $r^2 = 0.934$, $p < 0.001$). Data shown are from counts by KFD. Double-immunostained neurons were confirmed using a 40× objective lens (400× total magnification).

Table 1. Table showing rostrocaudal levels sampled for each subdivision and the grid surface area used.

Region	Rostrocaudal level (mm bregma)	Grid Size
mOFC	4.20	0.74 mm²
PrL	4.20	0.75 mm²
IL	3.20	1.00 mm²
Cg1	3.20	0.50 mm²
NAcbSh	1.20	0.60 mm²
MPA	—0.30	0.40 mm²
VP	—0.80	0.80 mm²
AIP	—1.50	0.50 mm²
MD	—1.88	0.35 mm²
PVA	—1.88	0.35 mm²
VPM	—3.14	0.50 mm²
VPL	—3.14	0.40 mm²
S1Tr	—3.14	0.40 mm²
DRD	—7.50	*
DRV	—7.50	*
DRD	—8.18	*
DRV	—8.18	*
DRVL	—8.18	*
DRC	—8.36	*
DRI	—8.36	*
DRC	—8.54	*
DRI	—8.54	*
DRC	—8.72	*
DRI	—8.72	*
LPBd	—9.34	0.10 mm²
LPBel	—9.34	0.08 mm²
LPBd	—9.52	0.10 mm²
LPBel	—9.52	0.08 mm²
LPBel	—9.70	0.08 mm²

* indicates regions counted in previous study

Cell counting, parabrachial and thalamic nuclei

The numbers of c-Fos-ir neurons were also counted in subdivisions located in regions not sampled in the initial study. We selected brain regions for study based on their predicted involvement in the thermoregulatory, discriminative, or affective components of warm thermosensation (Raison et al, 2015). Regions sampled included subdivisions of the lateral parabrachial nucleus (LPB), hypothalamus, thalamus, basal forebrain, and various regions in the cerebral cortex. Counts were taken at a total of twelve different rostrocaudal levels (4.2, 3.2, 1.2, −0.30, −0.80, −1.50, −1.88, −3.14, −9.34, −9.52, and −9.70 mm bregma) (Table 1).

Lateral parabrachial nucleus subdivisions included the lateral parabrachial nucleus, dorsal part (LPBd), and lateral parabrachial nucleus, external lateral part (LPBel). Hypothalamus subdivisions sampled include the medial part of the preoptic area (MPA). Thalamic subdivisions sampled include the medial and lateral posterior (VPM and VPL), posterior paraventricular (PVP), and mediodorsal (MD) thalamus. Basal forebrain regions sampled included the nucleus accumbens shell (NAcbSh) and ventral pallidum (VP). Regions sampled in the cerebral cortex include the medial orbitofrontal cortex (mOFC), infralimbic cortex (IL), prelimbic cortex (PrL), cingulate cortex (Cg1), agranular insular cortex (AIP) and the somatosensory cortex of the trunk (S1Tr). The rostrocaudal levels sampled at each subdivision, and the area (mm^2) sampled, are shown in Table 1. Rostrocaudal levels and anatomical boundaries of these subdivisions were based on comparison of immunostained sections with a stereotaxic rat brain atlas (Paxinos and Watson, 1998) and are illustrated in Figure 2. Subdivisions that were located on the midline

(MPA, PVP, MD, mOFC, IL, PrL, and Cg1) were counted on both the left and right sides of the midline and the cell counts were summed to give a total number of cells in each subdivision. Similarly, subdivisions that were bilateral structures (LPBd, LPBel, VPM, VPL, NAcbSh, VP, AIP, and S1Tr) were counted on both the left and right sides and the cell counts were summed to give a total number of cells in each subdivision. A 1.0 mm^2 grid embedded in the 10x objective was used to consistently examine the same surface area at a given rostrocaudal level. The grid area used to count the sampled brain section are shown in Table 1 and illustrated in Figure 2. The grid was placed at the same anatomical location on each individual sample to maintain consistent surface areas being sampled. C-Fos-ir cells that were located on the border of the grid were counted. Furthermore, round or oval-shaped cell nuclei with blue/black immunostaining darker than the background were counted as c-Fos-ir nuclei. One section from each rat at a given anatomical level was sampled. Cell counts were conducted using a 10× objective (100× total magnification) by an investigator (ASJ) blind to the assignment of treatment groups.

Spinoparabrachial pathway

Subdivisions of the LPB sampled included the lateral parabrachial nucleus, dorsal part (LPBd) and lateral parabrachial nucleus, external lateral part (LPBel). The numbers of c-Fos-ir neurons sampled were counted in the LPBd at two rostrocaudal levels (−9.34 and −9.52 mm bregma) and in the LPBel at three rostrocaudal levels (−9.34, −9.52, −9.70 mm bregma). These regions were selected for analysis based on previous studies showing thermosensitive neurons in the LPB (Nakamura and Morrison, 2010) at −9.16, −9.34, and −9.70 mm bregma. The subdivisions at −9.16 mm bregma were not analyzed because previous studies done in our lab sampled this region at −9.52 mm bregma instead of −9.16 mm bregma (Kelly et al, 2011). The different rostrocaudal levels of the LPBd and LPBel were summed to give LPB_{total} and $LPBel_{total}$ for each rat. The summed total for each subdivision was used for analysis.

Lateral spinothalamic pathway

Two subdivisions of the lateral thalamus were chosen for analysis (VPM and VPL), based on previous studies suggesting thermosensitive neurons in the ventrobasal thalamus projecting to multiple targets including the insula (Augustine, 1996), the thermosensory cortex (Craig et al, 1994, 1999), and

somatosensory cortex (Rolls et al, 2008). The subdivisions of the lateral ventrobasal thalamus sampled include the medial and lateral posterior thalamus (VPM and VPL) at −3.14 mm bregma. Because there were no c-Fos-ir cells observed at 100× magnification, a magnification of 400× was used to verify the absence of c-Fos-ir cells in these regions.

Medial spinothalamic pathway

Two subdivisions of the medial thalamus were chosen for analysis (MD and PVP) based on previous studies showing the role of the medial thalamus in depression circuitry (Price & Drevets, 2012). Furthermore, the midline thalamus has been shown to project to many cortical targets including the mOFC (Ray & Price, 1993), the anterior cingulate (Vogt et al, 1979), limbic regions (Vertes, 2004), and dorsal raphe nucleus (Krout et al, 2002). It has also been shown to receive input from various regions from the basal forebrain (Kuroda & Price, 1991). The subdivisions of the medial thalamus sampled include the mediodorsal and paraventricular posterior part (MD and PVP) thalamic nuclei at −1.88 mm bregma.

Cell counting, thermoregulatory, discriminative, and affective circuits

Thermoregulatory regions

Thermoregulatory regions are primarily located in the hypothalamus and, therefore, the medial preoptic nucleus (MPA) was chosen for analysis based on its thermoregulatory functions (Ray et al, 2001; Kumar, 2004; Nakamura and Morrison, 2008; Morrison and Nakamura, 2011). The MPA was sampled at a rostrocaudal level of −1.88 mm bregma.

Discriminative regions

One subdivision of the somatosensory cortex was chosen for analysis (S1Tr) based on many studies demonstrating the role of the ventrobasal thalamus projecting to the somatosensory cortex (Koralek et al, 1988). Furthermore, the insular cortex can be considered a discriminative region of the brain (Oshiro et al, 2009, Bornvold et al, 2002) and has been implicated in multiple studies for its

integration into limbic system circuitry (for review see Augustine,1996). The S1Tr was sampled at a rostrocaudal level of −3.14 mm bregma and the AIP was sampled at −1.50 mm bregma.

Affective/social regions

Many studies have suggested the dual role of somatosensory touch having a discriminatory component and an affective/social component (McGlone et al, 2014). To assess the role of warm ambient temperature on affective circuits, various regions associated with affect, emotion, pleasure and reward were chosen for analysis. Recent studies have proposed the presence of complex hedonic neural circuits (Berridge et al, 2011) which include regions like the mOFC and Cg1 in the forebrain (McGlone et al, 2014). Furthermore, regions in the basal forebrain, including the NAcbSh, and VP (Peciña et al, 2006), have been implicated as part of these hedonic circuits. Furthermore, the insula and limbic regions have been shown to integrate pain responses (Singer et al, 2009) and integrate memory and motivation to self-preservation (McLachlan, 2009). Therefore, the agranular insular cortex (AIP), infralimbic cortex (IL) and prelimbic cortex (PrL) were sampled as a model for pain and motivational behavior with ambient warm temperature. The rostrocaudal levels sampled at each of these subdivisions is shown in Table 1.

Statistical analysis

The T_{rec} data were analyzed using Student's *t*-test. Data for the cell counts were analyzed using analysis of variance (ANOVA) with repeated measures followed by post hoc analysis using Fisher's Protected Least Significant Difference (LSD) tests using PASW Statistics (17.0.2 for Windows, SPSS Inc., Chicago, IL, USA). A Greenhouse-Geisser correction epsilon (ε) was used for repeated measures analysis to correct for potential violation of the sphericity assumption.

As immunohistochemical procedures for the DR, spinoparabrachial, and spinothalamic pathways were conducted at different times, separate ANOVAs were conducted for the analysis of the DR and the spinoparabrachial/spinothalamic cell counts. The numbers of c-Fos-ir/Tph-ir (serotonergic) neurons in the DR, and the numbers of c-Fos-ir neurons in the spinoparabrachial/spinothalamic pathways, were analyzed separately using treatment group (two levels: RT and 37 °C) as a between-subjects factor and brain region as a within-subjects factor. Inter-rater reliability for the DR data set was calculated using

Pearson's correlation. Significance was accepted for the ANOVAs and post hoc Fisher's Protected LSD tests when $p < 0.05$.

Correlation analysis of T_{rec} and c-Fos expression in serotonergic neurons and in spinoparabrachial and spinothalamic pathways was conducted using Pearson's correlation between different nuclei. Outliers (2.0%; (DR), 1.4%; (spinoparabrachial/spinothalamic pathways)) were identified using Grubbs' test (Grubbs, 1969) and excluded. The RT group had a total of three outliers including one sample from the LPBd at −9.34 mm bregma, one sample from the MD at −1.88 mm bregma, and one from the VP at −0.80 mm bregma. The 37 °C group also had a total of three outliers including one from the LPBel at −9.52 mm bregma, one from the LPBel at −9.70 mm bregma, and one from the VP at −0.80 mm bregma. Replacement data for the repeated measures ANOVAs were calculated using the Petersen method (Petersen, 1985). Replacement data were not included in the post hoc analyses and are not represented in the tables of figures.

Image capture

Photomicrographs were taken using a Nikon 90i microscope and a Nikon DS-Fi1 digital camera, which was linked to a computer with NIS Elements 3.00 imaging software (A.G. Heinze Inc. Lake Forest, CA, USA). Photographic plates were prepared in CorelDraw for Windows 12.0 (Viglen Ltd., Wembley, UK).

Results

Rectal temperature

Rats exposed to the incubation chamber at 37 °C showed a 0.8 °C higher T_{rec} compared with rats exposed to the incubation chamber at room temperature. There was no difference in T_{rec} when comparing the RT and 37 °C groups at baseline five days prior to the test.

Dorsal raphe nucleus

c-Fos-ir serotonergic neurons in subdivisions of the DR

Exposure to 37 °C ambient temperature increased c-Fos expression in serotonergic neurons in the DR compared to room temperature (treatment × region $F_{(10,220)} = 4.46$, $p = 0.005$, $\varepsilon = 0.32$; treatment, $F_{(1,22)} = 8.37$, $p = 0.008$; region $F_{(10,220)} = 14.37$, $p = 0.001$, $\varepsilon = 0.32$; inter-rater reliability, $r^2 = 0.892$, $p = 0.001$). For a detailed description of these results, see (Hale et al, 2011). Warm ambient temperature increased c-Fos expression in serotonergic neurons in subdivisions of the DR. Post hoc Fisher's Protected LSD tests detected increases in the DRV at −7.46 mm and −8.18 mm bregma, the DRVL/VLPAG at −8.18 mm bregma, the DRC at −8.54 mm bregma, and in the DRI at each of the rostrocaudal levels sampled (−8.36, −8.54 and −8.72 mm bregma). The greatest numbers of c-Fos-ir serotonergic neurons were in the DRVL/VLPAG region (37 °C, 5.08 ± 1.49; RT, 1.91 ± 0.86).

Correlations

Based on data from rats exposed to either RT or 37 °C, the total numbers of c-Fos-ir serotonergic neurons in all of the subdivisions of the DR sampled in each rat were positively correlated with T_{rec} ($r^2 = 0.534$, $p = 0.007$). A positive correlation was also observed between T_{rec} and the numbers of c-Fos-ir serotonergic neurons in the DRVL/VLPAG ($r^2 = 0.631$, $p = 0.001$) and in the subset of DR subdivisions showing significant increases in c-Fos-ir serotonergic neurons ($r^2 = 0.56$, $p = 0.004$). The correlation between T_{rec} and the total numbers of c-Fos-ir serotonergic neurons in the subset of subdivisions of the DR that did not show significant warm temperature-induced increases in c-Fos expression did not reach statistical significance ($r^2 = 0.460$, $p = 0.024$) using Bonferroni adjusted alpha ($p = 0.0125$).

c-Fos-ir non-serotonergic cells in subdivisions of the DR

Exposure to warm ambient temperature increased c-Fos expression in non-serotonergic cells in the DR (treatment × region, $F_{(10,220)}$ = 2.659, p = 0.004, ε = 0.414; treatment, $F_{(1,22)}$ = 4.580, p = 0.044, region, $F_{(10,220)}$ = 43.501, p = 0.001, ε = 0.414; inter-rater reliability; r^2 = 0.862, p = 0.001). However this effect was not as widespread as that seen in serotonergic neurons. Post hoc tests revealed that the increases in c-Fos expression in non-serotonergic cells were restricted to the DRVL/VLPAG at −8.18 mm bregma and the DRC at −8.36 mm bregma.

Total numbers of serotonergic neurons in subdivisions of the DR

The numbers of TPH-ir neurons varied across the subdivisions of the DR sampled ($F_{(10,220)}$ = 55.619, p = 0.001, ε = 0.547; inter-rater reliability r^2 = 0.756, p = 0.001; Fig. 6). However, there were no effects of exposure to 37 °C, relative to RT controls, on the total numbers of TPH-ir neurons and there was no interaction between treatment and region.

Spinoparabrachial and spinothalamic pathways

Exposure to 37 °C ambient temperature increased c-Fos expression in components of the spinoparabrachial and spinothalamic pathways, compared to room temperature control conditions (treatment × region $F_{(17,374)}$ = 3.06, p = 0.024; treatment $F_{(1,22)}$ = 13.825, p = 0.001; region $F_{(17,374)}$ = 45.543, p = 0.001). Post hoc Fisher's protected LSD tests were performed and showed that warm ambient temperature increased c-Fos expression in multiple subdivisions of the spinoparabrachial and spinothalamic pathways (Figures 3-5).

C-Fos-ir neurons in subdivisions of the spinoparabrachial pathway

Post hoc tests detected whole-body heating induced increases in the LPBd at −9.34 mm and −9.52 mm bregma. Furthermore, there was an increase in the LPBel at −9.34 mm bregma, however, the LPBel at −9.52 mm and −9.70 mm bregma did not show increases in c-Fos-ir cells. When counts for the LPBd and LPBel were combined between rostrocaudal levels ($LPBd_{total}$ and $LPBel_{total}$), there were significant increases in c-Fos-ir cells after exposure to 37 ºC ambient warm temperature in the $LPBd_{total}$,

but not the $LPBel_{total}$ (Figure 3). Regions hypothesized to follow a spinoparabrachial pathway include the thermoregulatory regions (MPA). The MPA nucleus in the hypothalamus showed increased c-Fos-ir cells after exposure to 37 ºC warm ambient temperature. The greatest numbers of c-Fos-ir cells were in the LPBd subdivision after exposure to warm ambient temperature (see photomicrographs of these regions in Figure 6).

C-Fos-ir neurons in subdivisions of the lateral spinothalamic pathway

Post hoc tests were did not detect any differences in the VPM and VPL between conditions because neither region contained c-Fos-ir cells (Figure 4). Regions hypothesized to follow a lateral spinothalamic pathway include discriminative regions (S1Tr and AIP). Both the S1Tr and the AIP had detectable increased in the numbers of c-Fos-ir cells after exposure to 37 ºC warm ambient temperature (see photomicrographs of these regions in Figure 6).

C-Fos-ir neurons in subdivisions of the medial spinothalamic pathway

Post hoc tests detected increases in the more medial subdivisions of the thalamus and hypothalamus. Both the MD and PVP showed increased c-Fos-ir cells after exposure to 37 ºC warm ambient temperature (Figure 5). Regions hypothesized to follow a medial spinothalamic pathway include prefrontal (mOFC, PrL, IL, and Cg1) and basal forebrain areas (NAcbSh and VP). The mOFC bregma showed a strong increase in c-Fos-ir cells. Less strong but still detectable increases were seen in the IL. Post hoc tests did not detect increases in c-Fos-ir cells after exposure to 37 ºC warm ambient temperature in the PrL and Cg1. In the basal forebrain, post hoc tests revealed decreases in c-Fos-ir cells in the VP compared to RT controls. There was minimal immunoreactivity in the VP. Although there were decreases in the VP, the post hoc tests did not detect increases in the NAcbSh (see photomicrographs of these regions in Figure 6).

Correlations

Rectal temperature

Based on data from rats exposed to either RT or 37 °C, the numbers of c-Fos-ir neurons in a couple of the subdivisions sampled were positively correlated with T_{rec} (Figure 7). These include the $LPBd_{total}$ (r^2 = 0.726, p < 0.001; Figure 7A), and the mOFC (r^2 = 0.440, p = 0.032; Figure 7C). In contrast, the VP was negatively correlated with T_{rec} (r^2 = −0.639, p = 0.001; Figure 7B).

Spinoparabrachial pathway

Based on data from rats exposed to either RT or 37 °C, the numbers of c-Fos-ir neurons in the $LPBd_{total}$ positively correlated with the summed total of all of the different DR subdivisions (Table 2; Figure 8). The $LPBd_{total}$ was also positively correlated with a couple regions in the cortex: the mOFC (r^2 = 0.528, p = 0.011) and the IL (r^2 = 0.426, p = 0.048) (Table. 3). Furthermore, it should be noted that the $LPBel_{total}$ was not correlated with any other subdivision sampled except the LPBd at −9.34 & −9.52 mm bregma and $LPBd_{total}$. The DRI was also positively correlated with the AIP (r^2 = 0.591, p = 0.001).

Table 2. Table showing correlations (r^2) between DR and LPB subdivisions after exposure to 37°C ambient temperature.

					Region			
Region	**Temp**	**DRD_total**	**DRV_total**	**DRVL_total**	**DRC_total**	**DRI_total**	**LPBd_total**	**LPBel_total**
Temp	1.000	0.508*	0.541**	0.631**	0.421*	0.350	0.726**	0.349
DRD_total	0.508*	1.000	0.634**	0.800**	0.775**	0.600**	0.677**	0.348
DRV_total	0.541**	0.634**	1.000	0.805**	0.687**	0.672**	0.552**	0.235
DRVL_total	0.631**	0.800**	0.805**	1.000	0.866**	0.749**	0.748**	0.316
DRC_total	0.421*	0.775**	0.687**	0.866**	1.000	0.758**	0.677**	0.351
DRI_total	0.350	0.600**	0.672**	0.749**	0.758**	1.000	0.674**	0.258
LPBd_total	0.726**	0.677**	0.552**	0.748**	0.677**	0.674**	1.000	0.567*
LPBel_total	0.349	0.348	0.235	0.316	0.351	0.258	0.567*	1.000

*P<0.05, **P<0.01, Pearson 2-tailed Correlation.

Medial spinothalamic pathway

Both medial spinothalamic subdivisions sampled, the MD and PVP, were strongly correlated with one another (r^2 = 0.857, p < 0.001). In contrast to the LPBd, neither region was correlated with the DR with the exception of the MD with the DRV_{total} (r^2 = 0.449, p = 0.032). Although not correlated with the DR, the MD and PVP were positively correlated with many of the same structures in the cortex, hypothalamus, and basal forebrain (Table 3; Figure 9). The MD was strongly correlated with the mOFC (r^2 = 0.857, p < 0.001), the Cg1 (r^2 = 0.559, p = 0.006), and the S1Tr (r^2 = 0.539, p = 0.008) in the cortex and the MPA (r^2

= 0.675, $p < 0.001$) in the hypothalamus. It was also correlated with the NAcbSh ($r^2 = 0.438$, $p = 0.036$) in the basal forebrain. The PVP is similarly correlated with the same subdivisions as the MD with the exception that it was also correlated with the IL ($r^2 = 0.431$, $p = 0.033$) (Table 3; Figure 9). The IL was also positively correlated with the mOFC ($r^2 = 0.588$, $p = 0.003$) (Figure 10). Although neither medial thalamic subdivision was correlated with the PrL, it should be noted that the NAcbSh was strongly correlated with the PrL ($r^2 = 0.602$, $p = 0.002$) (Figure 10). The NAcbSh was also correlated with the mOFC ($r^2 = 0.554$, $p = 0.005$), IL ($r^2 = 0.609$, $p = 0.002$), and Cg1 ($r^2 = 0.516$, $p = 0.010$) which are all implicated in hedonic circuitry (Pecina et al, 2006; Berridge and Kringelbach, 2011). Lastly, it is important to note that multiple cortical structures were positively correlated with the MPA, a thermoregulatory region including the S1Tr ($r^2 = 0.713$, $p < 0.001$; Figure 10), Cg1 ($r^2 = 0.779$, $p < 0.001$; Figure 10) and mOFC ($r^2 = 0.625$, $p = 0.001$; Figure 10).

Lateral spinothalamic pathway

Both groups of rats exposed to RT and 37 °C did not contain c-Fos-ir cells in the ventrobasal thalamic nuclei. Therefore, they were not correlated with anything as c-Fos-ir cells were absent in both subdivisions sampled in the lateral thalamus.

Table 3. Correlations (r^2) between nuclei along the spinoparabrachial, medial spinothalamic, and lateral spinothalamic tracts and cortical regions after exposure to 37°C ambient temperature.

	Region															
Region	**Temp**	**mOFC**	**PrL**	**IL**	**Cg1**	**NAcbSh**	**MPA**	**VP**	**AIP**	**MD**	**PVP**	**VPM**	**VPL**	**S1Tr**	**LPBd_total**	**LPBel_total**
Temp	1.000	0.440*	-0.086	0.243	-0.005	-0.115	0.188	-0.639**	0.114	0.395	0.191	C	C	0.023	0.726**	0.349
mOFC	0.440*	1.000	0.341	0.588**	0.482*	0.554**	0.625**	-0.153	0.175	0.850**	0.667**	C	C	0.473*	0.528*	0.320
PrL	-0.086	0.341	1.000	0.126	0.092	0.602**	0.149	0.114	0.260	0.122	-0.006	C	C	0.227	0.268	0.039
IL	0.243	0.588**	0.126	1.000	0.661**	0.609**	0.573**	-0.141	0.284	0.331	0.437*	C	C	0.483*	0.426*	0.303
Cg1	-0.005	0.482*	0.092	0.661**	1.000	0.516**	0.779**	0.051	0.198	0.559**	0.628**	C	C	0.725**	0.030	0.006
NAcbSh	-0.115	0.554**	0.602**	0.609**	0.516**	1.000	0.614**	0.040	0.243	0.438*	0.452*	C	C	0.508*	0.157	0.134
MPA	0.188	0.625**	0.149	0.573**	0.779**	0.614**	1.000	-0.226	0.197	0.675**	0.719**	C	C	0.713**	0.265	0.270
VP	-0.639**	-0.153	0.114	-0.141	0.051	0.040	-0.226	1.000	0.097	-0.189	-0.032	C	C	-0.020	-0.392	-0.306
AIP	0.114	0.175	0.260	0.284	0.198	0.243	0.197	0.097	1.000	0.093	0.190	C	C	0.321	0.291	-0.123
MD	0.395	0.850**	0.122	0.331	0.559**	0.438*	0.675**	-0.189	0.093	1.000	0.857**	C	C	0.539**	0.270	0.090
PVP	0.191	0.667**	-0.006	0.437*	0.628**	0.452*	0.719**	-0.032	0.190	0.857**	1.000	C	C	0.567**	0.177	0.132
VPM	C	C	C	C	C	C	C	C	C	C	C	C	C	C	C	C
VPL	C	C	C	C	C	C	C	C	C	C	C	C	C	C	C	C
S1Tr	0.023	0.473*	0.227	0.483*	0.725**	0.508*	0.713**	-0.020	0.321	0.539**	0.567**	C	C	1.000	0.173	0.012
LPBd_total	0.726**	0.528*	0.268	0.426*	0.030	0.157	0.265	-0.392	0.291	0.270	0.177	C	C	0.173	1.000	0.567*
LPBel_total	0.349	0.320	0.039	0.303	0.006	0.134	0.270	-0.306	-0.123	0.090	0.132	C	C	0.012	0.567*	1.000

*P<0.05, **P<0.01, Pearson 2-tailed Correlation. C = cannot be calculated because at least one pf the variables is constant.

Discussion

Whole-body heating increased c-Fos expression in pathways involved in thermoregulatory, discriminative, and affective responses. We found that exposure to 37 ºC ambient warm temperature for 105 minutes provided stimulation to a variety of different brain nuclei that have widely different physiological functions. The MPA which is a primary thermoregulatory center in the hypothalamus responded with a greater than 300% increase in c-Fos-ir cells after exposure to warm ambient temperature compared to RT controls. Furthermore, the AIP, which is a major discriminative nucleus, responded with a greater than 200% increase in c-Fos-ir cells in the warm treatment compared to room temperature. Lastly, the mOFC, which is a major affective nucleus, responded with a nearly 400% increase in c-Fos-ir cells after the warm treatment compared to room temperature. These are just a few of many nuclei that show the role of whole-body heating on the multimodal circuits in the brain (Figures 3-5). Although warm ambient temperature provides input to the brain to a variety of different nuclei, the pathways that the stimulus takes to these regions is different. We found evidence that the discriminative component of whole-body heating follows a spinoparabrachial pathway while the thermoregulatory and affective components follow a medial spinothalamic pathway. On top of this, we found that the lateral spinothalamic pathway is not activated during exposure to ambient warm temperature. With all pathways considered, our data suggest that there are multiple afferent pathways relaying signals of cutaneous warmth to neural systems involved in thermoregulatory, discriminative, and affective brain circuits, including neuromodulatory input to these forebrain systems mediated by a spinoparabrachial activation of brainstem serotonergic systems.

Thermoregulatory component of whole-body heating

Preventing body temperature from reaching the hyperthermic range is one the most important homeostatic functions. Therefore, understanding the central mechanism of how increases in core body temperature are regulated is an important topic in neuroscience. Previous studies have demonstrated a spinoparabrachial pathway input to the brain thermoregulatory command center (Bratincsak & Palkovits, 2004; Nakamura & Morrison, 2008; Nakamura & Morrison, 2010; Morrison & Nakamura, 2011). We were unable to detect a correlation between the activation of the LPBd and MPA. Although not conclusive, this

finding suggests that there are other factors contributing to activation of the MPA following whole-body heating, that have not been accounted for. Although our result is conflicting with previous studies, it has been shown before that the MPA receives widespread input from various regions of the brain including the NAcbSh, IL, PVP (Simerly & Swanson, 1986) and more recently the Cg1 and mOFC (Farrell et al, 2013). Thus, it is possible that there is a descending pathway from the cortex is providing the primary stimulus for the MPA (Farrell et al, 2013) when exposed to warm innocuous temperatures while the spinoparabrachial pathway plays a modulatory role. Perhaps we did not see a correlation between the LPBd and the MPA because exposure to warm ambient temperature for 105 minutes was not long enough to require a major thermoregulatory response compared to an exposure of 240 minutes in previous studies (Nakamura & Morrison, 2010). If this is the case, it would suggest that the spinoparabrachial pathway would be, in effect, a neuromodulatory thermoregulatory pathway that provides a more robust homeostatic response when needed while the medial spinothalamic pathway provides the primary stimulus. There is also evidence that the MPA itself is thermosensitive and therefore, does not necessarily require input from either pathway (Boulant, 2000). Future studies that selectively lesion the different nuclei in the spinothalamic and spinoparabrachial pathway should be done to assess their role in thermoregulation.

Discriminative component of whole-body heating

Understanding the mechanisms behind sensory discrimination is integral to studying affective motivation because how you perceive sensory information will ultimately lead to how you feel about it (Craig, 2003). Contrary to the belief that discriminative aspects of thermosensation are mediated by the lateral spinothalamic pathway projecting to the ventrobasal thalamus, our findings suggest that the discriminative aspects of sensation during passive whole-body heating follows a spinoparabrachial pathway. Although there was not a correlation between the LPBd and AIP, both were strongly correlated with the DRI. Thus, it is possible that AIP activation follows a spinoparabrachial pathway through the DR. The posterior insula is primarily responsible for producing a relevant emotion in the context of discriminating painful sensations (Craig, 2009; Singer, 2009). The insula itself is merely a discriminative

region because it just senses pain (Raison, 2015), however, there are studies that have proposed its role in projecting to affective circuitry (Singer et al, 2004).

Previous studies have shown the differential AIP activation after being exposed to both innocuous and noxious warm temperatures (Craig et al, 2000; Moulton et al, 2004). This being said, it may be an anticipatory response to pain that may occur in the near future as body temperature increases. Alternatively, it may be thought of as a safety signal. The LPBd may be activating the DRI which in turn projects to the AIP as a safety signal. In order for this safety switch to work properly, the discriminative function of the insula would have to be inhibited. We propose that projections from the insula are inhibited in other regions by the spinoparabrachial pathway; however, this hypothesis needs to be investigated in future studies.

In contrast to the insula, our results suggest that the somatosensory cortex follows a medial spinothalamic pathway because the S1Tr was strongly correlated with both the MD and PVP. This is inconsistent with many studies proposing that the somatosensory cortex is primarily activated from the lateral spinoparabrachial pathway signaling via the ventrobasal thalamus (Burton et al, 1970; Hellon & Misra, 1973; Jahns, 1975; Morimoto et al, 1986). However, we found no activation in the ventrobasal thalamus. It is possible that the somatosensory cortex receives input from the lateral spinothalamic pathway when introduced to a thermal and mechanical stimuli combined. Most studies have demonstrated this connection with the use of heat applied to the skin using stimuli that involve mechanosensory stimulation (Burton et al, 1970; Hellon & Misra, 1973; Kahnds, 1975; Morimoto et al, 1986 Zhang & Oppenhiemer, 2000; Zhang et al, 2006) as opposed to passive whole-body heating used in this study. The fact that the somatosensory cortex can be activated by a different pathway when there is no mechanical stimulation points to another interesting dynamic of the discriminative sensory response to warm ambient temperature. These findings suggest that warm ambient heat should be classified as its own distinct stimulus as opposed to classifying it as a sense of warm mechanical touch in the traditional sense. This also provides interesting implications for the way we view sensory stimuli. Though warm innocuous touch and innocuous passive whole-body heating are both similar in nature, they signal to the brain by overlapping but distinct pathways.

It is also important to note that the S1Tr was correlated with many other affective regions including the mOFC, Cg1, and IL. In this way, ambient warm temperature may also be considered an affective somatosensory stimulus (Bushnell et al, 1999) that influences discriminative regions, such as the S1Tr, following a descending pathway from regions such as the mOFC, Cg1, and IL. This would not be the first time that descending pathways have been observed (Farrell et al, 2013), and future studies should be done to better understand the mechanism behind these novel pathways. Lastly, the correlation between the somatosensory cortex and thermoregulatory MPA nucleus was expected. The MPA requires modulation from discriminative components in order to produce a balanced response. This is a protective mechanism to ensure that the body does not overshoot its normal homeostatic range.

These findings contribute to the need for a paradigm shift in the way we think of sensory information processed in the brain. Current studies focus on the thalamus as the converging point for much of the sensory information; however, the lateral parabrachial nucleus is likely to be involved in sensory integration through stimulation of serotonergic systems as well as direct projections to thermoresponsive pathways. Perhaps the role of the lateral parabrachial nucleus in sensory discrimination is unique to warm ambient temperature which is not the traditional idea of sensory stimulus (ie mechanical touch, taste, smell, sight, and hearing). Nonetheless, our findings contribute to the emerging evidence for the spinoparabrachial pathway as an important sensory integration center. Furthermore, the absence of activation of the ventrobasal thalamus coupled with the activation somatosensory cortex provides interesting implications in the way environmental stimuli are signaled to the brain.

Affective/social component of whole-body heating

Although understanding the role of whole-body heating in thermoregulation and discriminatory sensation is important, its integral role in affective function provides the most practical use in a clinical setting. Depressed patients are often associated with decreased positive affect and increased negative affect, resulting in an emotional state that can largely be attributed to the dysregulation of neural pathways involved in emotion, feeling, and affect (for review see Gross, 1998). Many studies have shown the function of serotonin on cognitive and affective neural circuits involved in overall mood (Arango et al,

2002; Brown and Hariri, 2006; Dayan and Huys, 2009), which makes the dorsal raphe nucleus an important component in the onset of MDD. Our study demonstrates the potential for whole-body heating to stimulate certain aspects of these neural circuits hypothesized in previous literature (Raison et al, 2015). We found subdivisions of the DR and multiple affective cortical structures involved in emotional, motivational, and affective behaviors were activated after exposure to warm ambient innocuous temperature.

Our results ultimately show an interplay between many anatomically and functionally distinct nuclei (Figure 11). One of the most important findings in our study is the robust correlation between the LPBd and each of the subdivisions of the DR. Although the LPB is known to give rise to glutamatergic input to the DR (Lee et al, 2003), this is the first study to suggest that whole-body heating activates this parabrachial-raphe pathway. Different subdivisions of the DR give rise to different physiological and behavioral processes (Hale et al, 2013). The DRV is likely to contain a sensorimotor function (Greenwood et al, 2005). The DRD and DRC have been implicated in stress- and anxiety-related responses (Grahn et al, 1999; Abrams et al, 2005; Gardner et al, 2005; Amat et al, 2005; Bouwknecht et al, 2007). The DRVL and VLPAG are likely to contain an autonomic nervous system function (Kerman et al, 2006), and the DRI projects to forebrain targets that are likely involved in mediating antidepressant effects (Lowry et al, 2007). The fact that the LPBd projects to the subdivisions of the DR supports our hypothesis that the signal from warm ambient temperature follows a spinoparabrachial pathway to the DR. This would also suggest that whole-body heating serves to stimulate the proposed physiological and behavioral functions of the DR proposed in recent literature (for review, see Hale and Lowry, 2011). Although our data suggest that DR activation by whole-body heating follows a spinoparabrachial pathway, we did not see many correlations between DR subdivisions and cortical structures with the exception of the DRV with the mOFC and the DRI with the AIP. This is inconsistent with many studies showing the afferent and efferent projections between the DR and many forebrain and brainstem structures (Peyron et al, 1997; O'Hearn &Molliver, 1984; Swanson, 1982). It is possible that these results were achieved because of the unique stimulus that is passive whole-body heating. Many studies demonstrating the physiological and behavioral functions of the DR have not used warm ambient temperature as a stimulus so it is possible that the warm sensations following the spinoparabrachial pathway is inhibiting cortical structures, rather

than activating them. This could partially explain our results, although there is no hard evidence to suggest that is the case and this should be further investigated. Although activation in the DR itself is not correlated with activation of most cortical structures, it should be noted that the spinoparabrachial pathway may directly influence forebrain structures itself. The LPBd was positively correlated with both the mOFC and the IL suggesting that whole-body temperature increases are potentially signaled to affective cortical structures without going through the DR. So far as we are aware, there have not been any studies showing direct affective input from the LPBd, however, some studies have shown the reverse with affective regions in the primate medial prefrontal cortex providing descending activation to the LPBd (Chiba et al, 2001). Taken together, the DR activation following a spinoparabrachial pathway along with the possibility of the LPBd projecting to affective structures elucidates the potential for whole-body heating to produce antidepressant effects following a spinoparabrachial pathway. Further studies should be conducted investigating the lack of correlations between the DR to affective cortical structures following exposure to warm innocuous temperature stimuli and the emerging possibility of the interplay of descending affective cortical pathways on the spinoparabrachial pathway.

An interesting implication from this study is the functional redundancy of anatomically distinct neural pathways converging on the same functionally distinct nuclei (Figure 11). Both spinoparabrachial and spinothalamic pathways are projecting to many of the same affective nuclei. One specific nucleus that is involved in both the spinothalamic and spinoparabrachial pathways is the mOFC (Chiba et al, 2001; Leonard, 1969; Cavada et al, 2000; Price & Drevets, 2012) (Table 3). Moreover, the mOFC contained the most correlations with other cortical regions which confirm the functional importance of this particular forebrain region (Kringelbach & Rolls, 2004; Roll, 2004). The mOFC is important for both value guided and outcome guided behavior. When faced with a decision, it is involved in processing the reward and emotions involved with a given situation. This suggests that warm ambient temperature stimulated a region in the brain that classified the warm sensation as rewarding. The mOFC was one of the few cortical targets that was correlated with regions in the DR. It was correlated with the DRV, which is associated with motor function and learning and memory (for review, see Lowry et al, 2008), suggesting that there is motivation behind behavior associated whole-body heating because it is rewarding for the body. Other affective regions that were correlated with the mOFC included the anterior cingulate,

infralimbic, and the nucleus accumbens shell. The anterior cingulate is involved in emotional processing (for review, see Bush et al, 2000). The infralimbic cortex is primarily involved in inhibition of various affective nuclei (Vidal-Gonzalez, 2006). The nucleus accumbens shell is involved in motivational salience of reward and reinforcement (for review, see Salamone & Correa, 2002; Pecina et al, 2006). Furthermore, all of these affective nuclei share a common factor in the fact that they were all positively correlated with the mediodorsal thalamus. This being said, it is likely that these hedonic affective are projecting to one another (Pecina et al, 2006; Berridge et al, 2011), while also receiving initial input from a medial spinothalamic pathway (Krettek & Price, 1977). Our data demonstrate a medial spinothalamic-mOFC pathway through which warm temperature modulates affect. It is unlikely that the MD-mOFC modulates affective nuclei in an equivalent manner and further studies should be conducted investigating the efferent and afferent relationship between cortical structures.

It is also important to point out that the mOFC is correlated with thermoregulatory, discriminative, and affective circuits. This would suggest that the mOFC monitors value and outcomes based on homeostatic, discriminative, and affective relayed information. However, given the multimodal stimulation of warm ambient heating, it is important to note that the interplay between thermoregulatory, discriminatory, and affective components of whole-body heating may all contribute the potential treatment for major depressive disorder (MDD), though future studies would need to be done to investigate the modulatory role of each component on depression circuitry.

Conclusion

This study calls for a paradigm shift in the way we view signals to the brain and how they are integrated into neural circuits involved in depression. Previous studies have suggested a primary role of the lateral spinothalamic pathway in sensory discrimination and a spinoparabrachial pathway in thermoregulatory responses to innocuous warm temperature; however, our study has illustrated novel pathways through which warm ambient temperature signals to the brain which have the potential to provide antidepressant effects. As mentioned, warm ambient temperature as a stimulus has not received extensive investigation in neuroscience literature, and it is possible that these results were attained due to the unique multimodal nature of innocuous warm temperature on mammalian physiology (Hanusch et al, 2013). Nonetheless, warm ambient temperature activates brainstem serotonergic systems that have long been implicated in depressogenic circuitry and also activates cortical structures such as the mOFC and PrL that are known to have low activity in major depressive disorder (MDD) (Raison et al, 2015). Not only does it activate the DR, but our data suggest that passive whole-body heating activated affective cortical structures themselves through a medial spinothalamic pathway. Although not directly supporting the use of whole-body heating in providing antidepressant effects, these findings support the need for this novel mechanism to be investigated in human populations suffering with MDD. Given the widespread activation of affective circuits by whole-body heating, as shown in this study, further studies of the potential for whole-body heating to provide therapeutic effects in MDD and other psychiatric disorders that involve affective dysregulation are warranted

Acknowledgements

The author would like to acknowledge Dr. Christopher Lowry for his guidance, mentorship, and efforts enabling me to do this project. Furthermore, a special thanks to Kathleen Dady and Dr. Mathew Hale for their work in preparing the tissue and their assistance in getting this project started. I would also like to thank the Behavioral Neuroendocrinology Laboratory for graciously introducing me to the laboratory and for assisting me with many facets of this project. I would also like to express my gratitude for my committee members, Dr. David Sherwood and Dr. Rebecca Ciancanelli for taking the time to be a part of my defense. Finally, I would like to thank the University of Colorado Undergraduate Research Opportunities Program for funding me throughout the duration of this project.

References

1. Abrams, J. K., Johnson, *P*. L., Hay-Schmidt, A., Mikkelsen, J. D., Shekhar, A., & Lowry, C. A. (2005). Serotonergic systems associated with arousal and vigilance behaviors following administration of anxiogenic drugs. *Neuroscience*, *133*(4), 983-997.

2. Amat, J., Baratta, M. V., Paul, E., Bland, S. T., Watkins, L. R., & Maier, S. F. (2005). Medial prefrontal cortex determines how stressor controllability affects behavior and dorsal raphe nucleus. *Nature neuroscience*, *8*(3), 365-371.

3. Arango, V., Underwood, M. D., & Mann, J. J. (2002). Serotonin brain circuits involved in major depression and suicide. *Progress in brain research*, *136*, 443-453.

4. Augustine, J. R. (1996). Circuitry and functional aspects of the insular lobe in primates including humans. Brain Res. *Brain Res. Rev*. 22, 229–244.

5. Azmitia, E.C., Gannon, *P*.J. (1986). Anatomy of the serotonergic system in the primate and sub-primate brain. Adv. *Neurol*. 43, 407–468.

6. Balaban, C.D., Ogburn, S.W., Warshafsky, S.G., Ahmed, A., Yates, B.J. (2014). Identification of neural networks that contribute to motion sickness though principal components analysis of fos labeling induced by galvanic vestibular stimulation. *PloS one,* 9, 1

7. Barton, D. A., Esler, M. D., Dawood, T., Lambert, E. A., Haikerwal, D., Brenchley, C., … & Lambert, G. W. (2008). Elevated brain serotonin turnover in patients with depression: effect of genotype and therapy. *Archives of General Psychiatry*, *65*(1), 38-46.

8. Bernard, J.F., Dallel, R., Raboisson, *P*., Villanueva, L. & Le Bars, D. (1995). Organization of the efferent projections from the spinal cervical enlargement to the parabrachial area and periaqueductal gray: a PHAL study in the rat. J. Comp*. Neurol*. 353, 480-505.

9. Berridge, K. C., & Kringelbach, M. L. (2011). Building a neuroscience of pleasure and well-being. Psychology of well-being, 1(1), 1-26.

10. Bornhövd, K., Quante, M., Glauche, V., Bromm, B., Weiller, C., & Büchel, C. (2002). Painful stimuli evoke different stimulus–response functions in the amygdala, prefrontal, insula and somatosensory cortex: a single-trial fMRI study. *Brain*, *125*(6), 1326-1336.

11. Boulant, J. A. (2000). Role of the preoptic-anterior hypothalamus in thermoregulation and fever. *Clinical infectious diseases*, *31*(Supplement 5), S157-S161.

12. Bouwknecht, J. A., Spiga, F., Staub, D. R., Hale, M. W., Shekhar, A., & Lowry, C. A. (2007). Differential effects of exposure to low-light or high-light open-field on anxiety-related behaviors: relationship to c-Fos expression in serotonergic and non-serotonergic neurons in the dorsal raphe nucleus. *Brain research bulletin*, *72*(1), 32-43.

13. Bratincsak, A., & Palkovits, M. (2004). Activation of brain areas in rat following warm and cold ambient exposure. *Neuroscience*, *127*(2), 385-397.

14. Bromet, E., Andrade, L. H., Hwang, I., Sampson, N. A., Alonso, J., De Girolamo, G., ... & Kessler, R. C. (2011). Cross-national epidemiology of DSM-IV major depressive episode. *BMC medicine*, *9*(1), 90.

15. Brown, S. M., & Hariri, A. R. (2006). Neuroimaging studies of serotonin gene polymorphisms: exploring the interplay of genes, brain, and behavior. *Cognitive, Affective, & Behavioral Neuroscience*, *6*(1), 44-52.

16. Burton, H., Forbes, D. J., & Benjamin, R. M. (1970). Thalamic neurons responsive to temperature changes of glabrous hand and foot skin in squirrel monkey. *Brain research*, *24*(2), 179-190.

17. Burstein, R., Jakubowski, M., Garcia-Nicas, E., Kainz, V., Bajwa, Z., Hargreaves, R., Borsook, D. (2010). Thalamic sensitization transforms localized pain into widespread allodynia. *Annals of neurology*, *68*(1), 81-91.

18. Bush, G., Luu, P., & Posner, M. I. (2000). Cognitive and emotional influences in anterior cingulate cortex. *Trends in cognitive sciences*, *4*(6), 215-222.

19. Bushnell, M. C., Duncan, G. H., Hofbauer, R. K., Ha, B., Chen, J. I., & Carrier, B. (1999). Pain perception: is there a role for primary somatosensory cortex?. *Proceedings of the National Academy of Sciences*, *96*(14), 7705-7709.

20. Cavada, C., Tejedor, J., Cruz-Rizzolo, R. J., & Reinoso-Suárez, F. (2000). The anatomical connections of the macaque monkey orbitofrontal cortex. A review. *Cerebral Cortex*, *10*(3), 220-242.

21. Cechetto, D. F., & Saper, C. B. (1987). Evidence for a viscerotopic sensory representation in the cortex and thalamus in the rat. *Journal of Comparative Neurology*, *262*(1), 27-45.

22. Cechetto, D.F., Standeart D.G. & Saper, C.B. (1985). Spinal and trigeminal dorsal horn projections to the parabrachial nucleus in the rat. J. Comp. *Neurol*. 240, 153-160.

23. Chiba, T., Kayahara, T., & Nakano, K. (2001). Efferent projections of infralimbic and prelimbic areas of the medial prefrontal cortex in the Japanese monkey, Macaca fuscata. *Brain research*, *888*(1), 83-101.

24. Craig, A. D. (2003). A new view of pain as a homeostatic emotion. *Trends in neurosciences*, *26*(6), 303-307.

25. Craig, A. B. (2009). How do you feel--now? The anterior insula and human awareness. *Nature Reviews Neuroscience*, (10), 59-70.

26. Craig, A. D., Bushnell, M. C., Zhang, E. T., and Blomqvist, A. (1994). A thalamic nucleus specific for pain and temperature sensation. *Nature* 372, 770–773.

27. Craig, A. D., Chen, K., Bandy, D., & Reiman, E. M. (2000). Thermosensory activation of insular cortex. *Nature neuroscience*, *3*(2), 184-190.

28. Craig, A. D., Zhang, E. T., and Blomqvist, A. (1999). A distinct thermoreceptive subregion of lamina I in nucleus caudalis of the owl monkey. J. Comp. *Neurol.* 404, 221–234.

29. Davis, K. D., Kwan, C. L., Crawley, A. *P*., & Mikulis, D. J. (1998). Functional MRI study of thalamic and cortical activations evoked by cutaneous heat, cold, and tactile stimuli. *Journal of Neurophysiology*, *80*(3), 1533-1546.

30. Dayan, *P*., & Huys, Q. J. (2009). Serotonin in affective control. *Annual review of neuroscience*, *32*, 95-126.

31. Drevets, W. C., Price, J. L., & Furey, M. L. (2008). Brain structural and functional abnormalities in mood disorders: implications for neurocircuitry models of depression. *Brain structure and function*, *213*(1-2), 93-118.

32. Farrell, M. J., Trevaks, D., Taylor, N. A., & McAllen, R. M. (2013). Brain stem representation of thermal and psychogenic sweating in humans. *American Journal of Physiology-Regulatory, Integrative and Comparative Physiology*, *304*(10), R810-R817.

33. Feil, K. & Herbert, H. (1995). Topographic organization of spinal and trigeminal somatosensory pathways to the rat parabrachial and Kolliker-Fuse nuclei. *J. Comp. Neurol*. 353, 506-528.

34. Gardner, K. L., Thrivikraman, K. V., Lightman, S. L., Plotsky, *P*. M., & Lowry, C. A. (2005). Early life experience alters behavior during social defeat: focus on serotonergic systems. *Neuroscience*, *136*(1), 181-191.

35. Gordon, C. J. (1990). Thermal biology of the laboratory rat. *Physiology & Behavior*, *47*(5), 963-991.

36. Grahn, R. E., Will, M. J., Hammack, S. E., Maswood, S., McQueen, M. B., Watkins, L. R., & Maier, S. F. (1999). Activation of serotonin-immunoreactive cells in the dorsal raphe nucleus in rats exposed to an uncontrollable stressor. *Brain research*, *826*(1), 35-43.

37. Greenwood, B. N., Foley, T. E., Day, H. E., Burhans, D., Brooks, L., Campeau, S., & Fleshner, M. (2005). Wheel running alters serotonin (5-HT) transporter, 5-HT 1A, 5-HT 1B, and alpha 1b-adrenergic receptor mRNA in the rat raphe nuclei. Biological Psychiatry, 57(5), 559-568.

38. Gross, J. J. (1998). The emerging field of emotion regulation: an integrative review. *Review of general psychology*, *2*(3), 271.

39. Hale, M.W., Stamper, C.E., Staub, D.R., Lowry, C.A. (2010). Urocortin 2 increases c-Fos expression in serotonergic neurons projecting to the ventricular/periventricular system. *Exp. Neurol.* 224, 271–281.

40. Hale, M. W., & Lowry, C. A. (2011). Functional topography of midbrain and pontine serotonergic systems: implications for synaptic regulation of serotonergic circuits*. Psychopharmacology*, 213(2-3), 243-264.

41. Hale, M. W., Dady, K. F., Evans, A. K., & Lowry, C. A. (2011). Evidence for in vivo thermosensitivity of serotonergic neurons in the rat dorsal raphe nucleus and raphe pallidus nucleus implicated in thermoregulatory cooling*. Experimental Neurology*, 227(2), 264-78.

42. Hale, M. W., Raison, C. L., & Lowry, C. A. (2013). Integrative physiology of depression and antidepressant drug action: Implications for serotonergic mechanisms of action and novel therapeutic strategies for treatment of depression. *Pharmacology & therapeutics*, 137(1), 108-118.

43. Hanusch, K. U., Janssen, C. H., Billheimer, D., Jenkins, I., Spurgeon, E., Lowry, C. A., & Raison, C. L. (2013). Whole-body hyperthermia for the treatment of major depression: associations with thermoregulatory cooling. *American Journal of Psychiatry*, *170*(7), 802-804.

44. Hellon, R. F., & Misra, N. K. (1973). Neurons in the ventrobasal complex of the rat thalamus responding to scrotal skin temperature changes. *The Journal of physiology*, *232*(2), 389-399.

45. Jahns, R. (1975). Types of neuronal responses in the rat thalamus to peripheral temperature changes. *Experimental brain research*, *23*(2), 157-166.

46. Keller, M. B., Lavori, P. W., Mueller, T. I., Endicott, J., Coryell, W., Hirschfeld, R. M., & Shea, T. (1992). Time to recovery, chronicity, and levels of psychopathology in major depression: a 5-year prospective follow-up of 431 subjects. *Archives of General Psychiatry*, *49*(10), 809-816.

47. Kelly, K. J., Donner, N. C., Hale, M. W., & Lowry, C. A. (2011). Swim stress activates serotonergic and nonserotonergic neurons in specific subdivisions of the rat dorsal raphe nucleus in a temperature-dependent manner. *Neuroscience,* 197, 251-268.

48. Kerman, I. A., Shabrang, C., Taylor, L., Akil, H., & Watson, S. J. (2006). Relationship of presympathetic-premotor neurons to the serotonergic transmitter system in the rat brainstem. *Journal of Comparative Neurology*, *499*(6), 882-896.

49. Koralek, K. A., Jensen, K. F., & Killackey, H. *P*. (1988). Evidence for two complementary patterns of thalamic input to the rat somatosensory cortex. *Brain research*, 463(2), 346-351.

50. Krettek, J. E., & Price, J. L. (1977). The cortical projections of the mediodorsal nucleus and adjacent thalamic nuclei in the rat. *Journal of Comparative Neurology*, *171*(2), 157-191.

51. Kringelbach, M. L., & Rolls, E. T. (2004). The functional neuroanatomy of the human orbitofrontal cortex: evidence from neuroimaging and neuropsychology. *Progress in neurobiology*, *72*(5), 341-372.

52. Krout, K. E., Belzer, R. E., & Loewy, A. D. (2002). Brainstem projections to midline and intralaminar thalamic nuclei of the rat. *Journal of Comparative Neurology*, 448(1), 53-101.

53. Kumar, V. M. (2004). Body temperature and sleep: are they controlled by the same mechanism?. *Sleep and Biological Rhythms*, 2(2), 103-124.

54. Kuroda, M., & Price, J. L. (1991). Synaptic organization of projections from basal forebrain structures to the mediodorsal thalamic nucleus of the rat*. Journal of comparative neurology*, 303(4), 513-533.

55. Lee, H. S., Kim, M. A., Valentino, R. J., & Waterhouse, B. D. (2003). Glutamatergic afferent projections to the dorsal raphe nucleus of the rat. *Brain research*, *963*(1), 57-71.

56. Leonard, C. M. (1969). The prefrontal cortex of the rat. I. Cortical projection of the mediodorsal nucleus. II. Efferent connections. *Brain research*, *12*(2), 321-343.

57. Lira, A., Zhou, M., Castanon, N., Ansorge, M. S., Gordon, J. A., Francis, J. H., ... & Gingrich, J. A. (2003). Altered depression-related behaviors and functional changes in the dorsal raphe nucleus of serotonin transporter-deficient mice. *Biological psychiatry*, *54*(10), 960-971.

58. Lowry, C. A., Hollis, J. H., De Vries, A., Pan, B., Brunet, L. R., Hunt, J. R., ... & Lightman, S. L. (2007). Identification of an immune-responsive mesolimbocortical serotonergic system: potential role in regulation of emotional behavior. *Neuroscience,* 146(2), 756-772.

59. Lowry, C.A., Lightman, S.L., Nutt, D.J. (2009). That warm fuzzy feeling: brain serotonergic neurons and the regulation of emotion. *J. Psychopharmacology*. 23, 392-400.

60. Lumpkin, E.A. & Caterina, M.J. (2007). Mechanisms of sensory transduction in the skin. *Nature* 445, 858-865.

61. Mann, J. J. (1999). Role of the serotonergic system in the pathogenesis of major depression and suicidal behavior. *Neuropsychopharmacology*, *21*, 99S-105S.

62. Mathers, C. D., & Loncar, D. (2006). Projections of global mortality and burden of disease from 2002 to 2030. *PLoS medicine*, *3*(11), e442.

63. McGlone, F., Wessberg, J., & Olausson, H. (2014). Discriminative and affective touch: sensing and feeling. *Neuron*, 82(4), 737-755.

64. McLachlan, R. S. (2009). A brief review of the anatomy and physiology of the limbic system. The Canadian journal of neurological sciences*. Le journal canadien des sciences neurologiques*, 36, S84-7.

65. Michelsen, K. A., Schmitz, C., & Steinbusch, H. W. (2007). The dorsal raphe nucleus—from silver stainings to a role in depression. *Brain research reviews*, *55*(2), 329-342.

66. Morimoto, A., Murakami, N. & Sakata, Y. (1988). Changes in hypothalamic temperature modulate the neuronal response of the ventral thalamus to skin warming in rats. *The Journal of physiology*, *398*(1), 97-108.

67. Morrison, S. F., & Nakamura, K. (2011). Central neural pathways for thermoregulation. *Frontiers in bioscience: a journal and virtual library*, *16*, 74.

68. Moulton, E. A., Keaser, M. L., Gullapalli, R. *P*., & Greenspan, J. D. (2005). Regional intensive and temporal patterns of functional MRI activation distinguishing noxious and innocuous contact heat. *Journal of neurophysiology*, *93*(4), 2183-2193.

69. Murray, C. J., & Lopez, a D. (1996). Evidence-based health policy--lessons from the Global Burden of Disease Study. *Science*, 274(5288), 740-3.

70. Nakamura, K., Morrison, S.F. (2008). A thermosensory pathway that controls body temperature. *Nat. Neurosci*. 11, 62-71.

71. Nakamura, K., & Morrison, S. F. (2010). A thermosensory pathway mediating heat-defense responses. *Proceedings of the National Academy of Sciences*, *107*(19), 8848-8853.

72. O'Hearn, E., & Molliver, M. E. (1984). Organization of raphe-cortical projections in rat: a quantitative retrograde study. *Brain research bulletin*, *13*(6), 709-726.

73. Oshiro, Y., Quevedo, A. S., McHaffie, J. G., Kraft, R. A., & Coghill, R. C. (2009). Brain mechanisms supporting discrimination of sensory features of pain: a new model. *The Journal of Neuroscience*, *29*(47), 14924-14931.

74. Raison, C. L. (2015). Cingulate and insula: the pain in the brain is not all the same. *Biological psychiatry*, *77*(3), 205.

75. Paxinos, G., Watson, C., (1998). The Rat Brain in Stereotaxic Coordinates, Fourth Edition. Academic Press, San Diego.

76. Peciña, S., Smith, K. S., & Berridge, K. C. (2006). Hedonic hot spots in the brain. *The Neuroscientist*, 12(6), 500-511.

77. Petersen, R.G. (1985). Design and analysis of experiments. Marcel Dekker, Inc., New York.

78. Peyron, C., Petit, J. M., Rampon, C., Jouvet, M., & Luppi, *P*. H. (1997). Forebrain afferents to the rat dorsal raphe nucleus demonstrated by retrograde and anterograde tracing methods. *Neuroscience*, *82*(2), 443-468.

79. Price, J.L., & Drevets, W.C. (2010). Neurocircuitry of mood disorders. *Neuropsychopharmacology.* 35(1), 192-216.

80. Price, J. L., & Drevets, W. C. (2012). Neural circuits underlying the pathophysiology of mood disorders. *Trends in cognitive sciences*, 16(1), 61-71.

81. Raison, C. L., Hale, M. W., Williams, L., Wager, T. D., & Lowry, C. A., 2015. Somatic influences on subjective well-being and affective disorders: the convergence of thermosensory and central serotonergic systems*. Frontiers in Psychology*, 5, 1580.

82. Ray, B. Mallick, H., & Kumar, V. M. (2001). Role of the medial preoptic area in thermal preference of rats. *Indian journal of physiology and pharmacology*, 45(4), 445-450.

83. Ray, J. *P*., & Price, J. L. (1993). The organization of projections from the mediodorsal nucleus of the thalamus to orbital and medial prefrontal cortex in macaque monkeys. *Journal of Comparative Neurology*, 337(1), 1-31.

84. Rolls, E. T. (2004). The functions of the orbitofrontal cortex. *Brain and cognition*, *55*(1), 11-29.

85. Rolls, E. T., Grabenhorst, F., and Parris, B. A. (2008). Warm pleasant feelings in the brain. *Neuroimage* 41, 1504–1513.

86. Sakowski, S. A., Geddes, T. J., Thomas, D. M., Levi, E., Hatfield, J. S., & Kuhn, D. M. (2006). Differential tissue distribution of tryptophan hydroxylase isoforms 1 and 2 as revealed with monospecific antibodies. *Brain research*, *1085*(1), 11-18.

87. Salamone, J. D., & Correa, M. (2002). Motivational views of reinforcement: implications for understanding the behavioral functions of nucleus accumbens dopamine. *Behavioural brain research*, *137*(1), 3-25.

88. Simerly, R. B., & Swanson, L. W. (1986). The organization of neural inputs to the medial preoptic nucleus of the rat. *Journal of Comparative Neurology*, *246*(3), 312-342.

89. Singer, T., Critchley, H. D., & Preuschoff, K. (2009). A common role of insula in feelings, empathy and uncertainty. *Trends in cognitive sciences*, 13(8), 334-340.

90. Singer, T., Seymour, B., O'Doherty, J., Kaube, H., Dolan, R. J., & Frith, C. D. (2004). Empathy for pain involves the affective but not sensory components of pain. *Science*, *303*(5661), 1157-1162.

91. Smith, J.E., Jansen, A.S., Gilbey, M.*P*., Loewy, A.D. (1998). CNS cell groups projecting to sympathetic outflow of tail artery: neural circuits involved in heat loss in the rat. *Brain Res*. 786, 153-164.

92. Steinbusch, H.W.M. (1984). Serotonin-immunoreactive neurons and their projections in the CNS. In: Björklund, A., Hökfelt, T. (Eds.), Classical Transmitters and Transmitter Receptors in the CNS. Elsevier Science Publishers B.V., Amsterdam, pp. 68–125.

93. Swanson, L. W. (1982). The projections of the ventral tegmental area and adjacent regions: a combined fluorescent retrograde tracer and immunofluorescence study in the rat. *Brain research bulletin*, *9*(1), 321-353.

94. Toth, I.E., Toth, D.E., Boldogkoi, Z., Hornyak, A., Palkovits, M., Blessing, W.W. (2006). Serotonin-synthesizing neurons in the rostral medullary raphe/parapyramidal region transneuronally labelled after injection of pseudorabies virus into the rat tail*. Neurochem*. Res. 31, 277-286.

95. Vertes, R. *P*. (2004). Differential projections of the infralimbic and prelimbic cortex in the rat. *Synapse*, 51(1), 32-58.

96. Vidal-Gonzalez, I., Vidal-Gonzalez, B., Rauch, S. L., & Quirk, G. J. (2006). Microstimulation reveals opposing influences of prelimbic and infralimbic cortex on the expression of conditioned fear. *Learning & memory*, *13*(6), 728-733.

97. Vogt, B. A., Rosene, D. L., & Pandya, D. N. (1979). Thalamic and cortical afferents differentiate anterior from posterior cingulate cortex in the monkey. *Science*, 204(4389), 205-207.

98. Walther, D. J., Peter, J. U., Bashammakh, S., Hörtnagl, H., Voits, M., Fink, H., & Bader, M. (2003). Synthesis of serotonin by a second tryptophan hydroxylase isoform. *Science*, *299*(5603), 76-76.

99. Yang, L. M., Hu, B., Xia, Y. H., Zhang, B. L., & Zhao, H. (2008). Lateral habenula lesions improve the behavioral response in depressed rats via increasing the serotonin level in dorsal raphe nucleus. *Behavioural brain research*, *188*(1), 84-90.

100 Zhang, X., Davidson, S., & Giesler, G. J. (2006). Thermally identified subgroups of marginal zone neurons project to distinct regions of the ventral posterior lateral nucleus in rats. *The Journal of neuroscience*, *26*(19), 5215-5223.

101 Zhang, Z. H., & Oppenheimer, S. M. (2000). Baroreceptive and somatosensory convergent thalamic neurons project to the posterior insular cortex in the rat. *Brain research*, *861*(2), 241-256

.

Figures

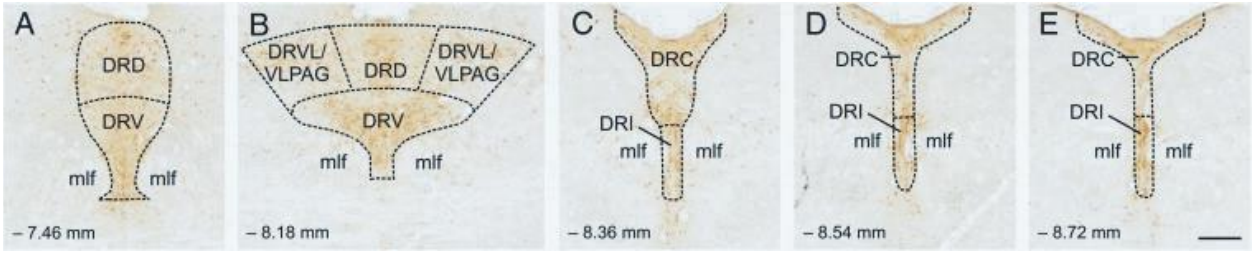

Figure 1. Low-power photomicrographs illustrating c-Fos/tryptophan hydroxylase (TPH)-immunostaining in 11 subdivisions of the dorsal raphe nucleus (DR) sampled in the previous study. The subdivisions of the DR are illustrated by dashed lines. For abbreviations, see *Abbreviations*. Scale bar: 500 μm.

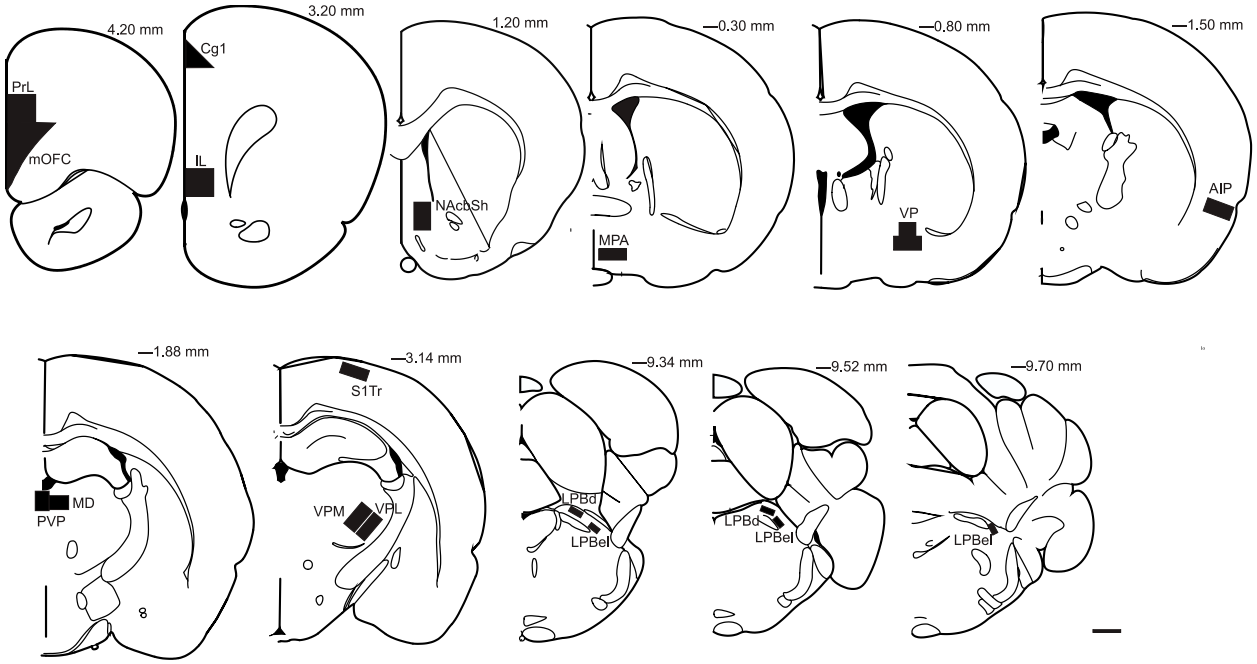

Figure 2. Line drawings (adapted from Paxinos and Watson, 1998) showing the 18 brain regions where c-Fos-ir nuclei were quantified. The shaded rectangles and triangles indicate the placement of the grids for counting c-Fos-ir cells. Shaded triangles were measured using a square grid and only half of a single grid's surface area was used along the hypotenuse of the region. Numbers above each diagram indicate the distance (in mm) from bregma. For abbreviations, see *Abbreviations.* Scale bar: 1,000 μm.

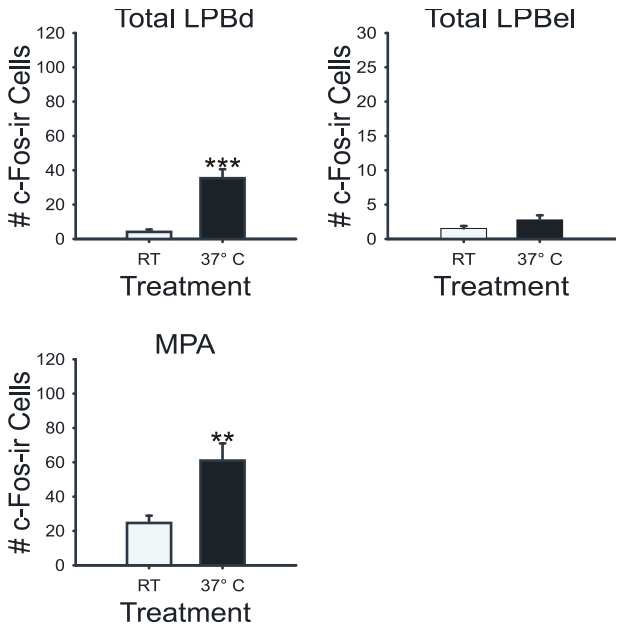

Figure 3. Exposure to 37 ºC ambient temperature for 105 minutes increased c-Fos expression within specific subdivisions in the parabrachial nucleus (LPBd and LPBel) and the thermoregulatory hypothalamus (MPA). Black bars represent the numbers of c-Fos-ir cells after exposure to warm ambient temperature, and white bars represent the numbers of c-Fos-ir cells after exposure to room temperature. See Table 1 for rostrocaudal level in mm bregma sampled (Paxinos & Watson, 1998). For abbreviations see *Abbreviations*. *$p < 0.05$, **$p < 0.01$, ***$p < 0.001$ versus RT control, Fisher's Protected LSD tests (LPBd, n = 11 for RT, n = 12 for 37 ºC; LPBel, n = 12 for RT, n = 10 for 37 ºC; MPA, n = 12 for RT, n = 12 for 37 ºC).

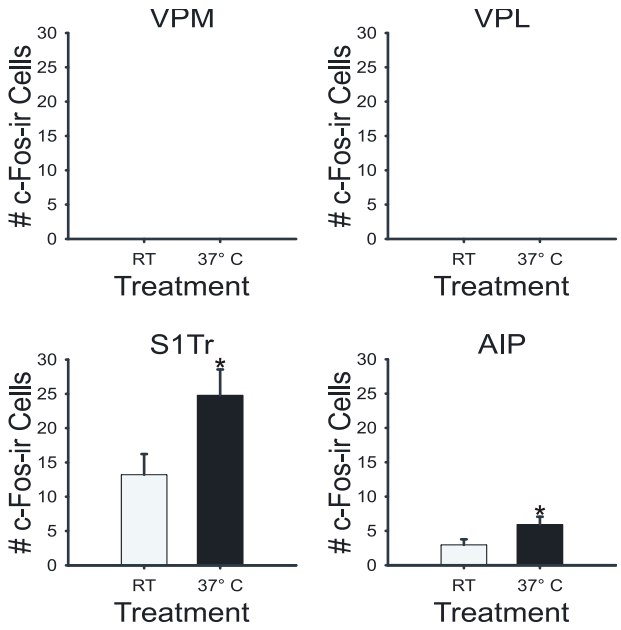

Figure 4. Exposure to 37 ºC ambient temperature for 105 minutes increased c-Fos expression within specific subdivisions in the lateral thalamus (VPM and VPL) and discriminative cerebral cortex (S1Tr and AIP). Black bars represent the numbers of c-Fos-ir cells after exposure to warm ambient temperature, and white bars represent the numbers of c-Fos-ir cells after exposure to room temperature. See Table 1 for rostrocaudal level in mm bregma sampled (Paxinos & Watson, 1998). For abbreviations see *Abbreviations*. *$p < 0.05$, **$p < 0.01$, ***$p < 0.001$ versus RT control, Fisher's Protected LSD tests (VPM, n = 12 for RT, n = 12 for 37 ºC; VPL, n = 12 for RT, n = 12 for 37 ºC; S1Tr, n = 12 for RT, n = 12 for 37 ºC; AIP, n = 12 for RT, n = 12 for 37 ºC)

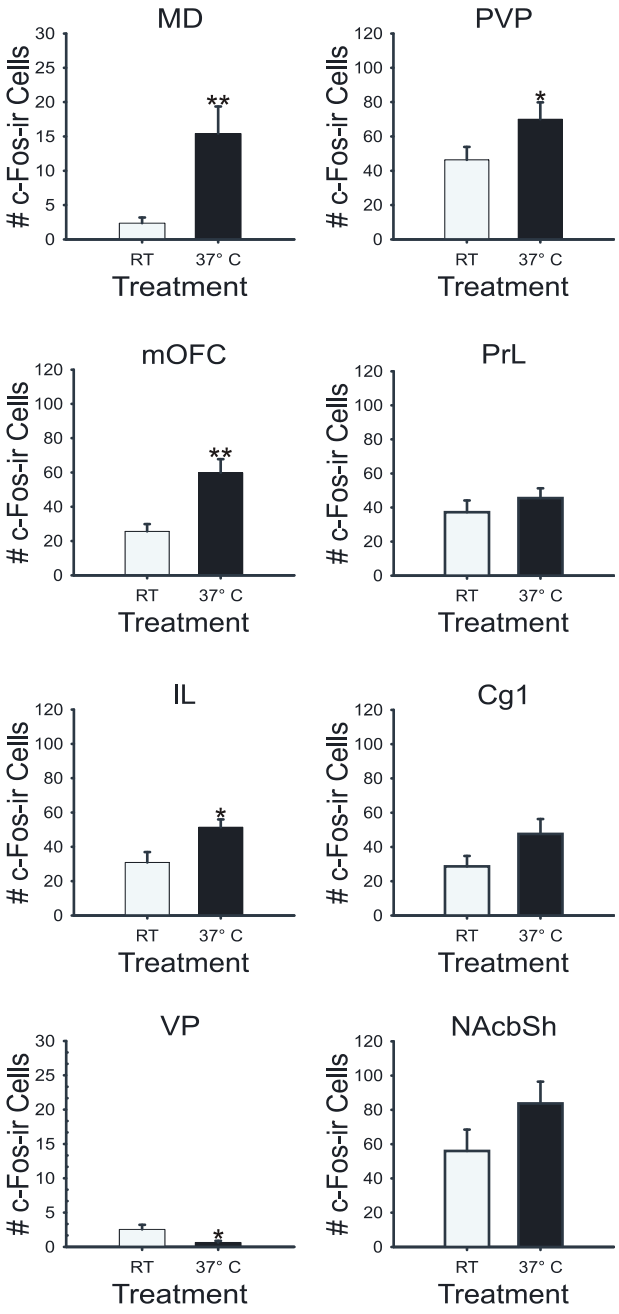

Figure 5. Exposure to 37 ºC ambient temperature for 105 minutes increased c-Fos expression within specific subdivisions in the medial thalamus (MD and PVP), frontal cortex (mOFC, PrL, IL, Cg1), and basal forebrain (VP and NAcbSh). Black bars represent the numbers of c-Fos-ir cells after exposure to warm ambient temperature, and white bars represent the numbers of c-Fos-ir cells after exposure to room temperature. See Table 1 for rostrocaudal level in mm bregma sampled (Paxinos & Watson, 1998). For abbreviations see *Abbreviations*. **p* < 0.05, ***p* < 0.01, ****p* < 0.001 versus RT control, Fisher's Protected LSD tests (MD, n = 11 for RT, n = 12 for 37 ºC; PVP, n = 12 for RT, n = 12 for 37 ºC; mOFC, n = 12 for RT, n = 12 for 37 ºC; PrL, n = 12 for RT, n = 12 for 37 ºC; IL, n = 12 for RT, n = 12 for 37 ºC; Cg1, n = 12 for RT, n = 12 for 37 ºC; VP, n = 11 for RT, n = 11 for 37 ºC; NAcbSh, n = 12 for RT, n = 12 for 37 ºC)

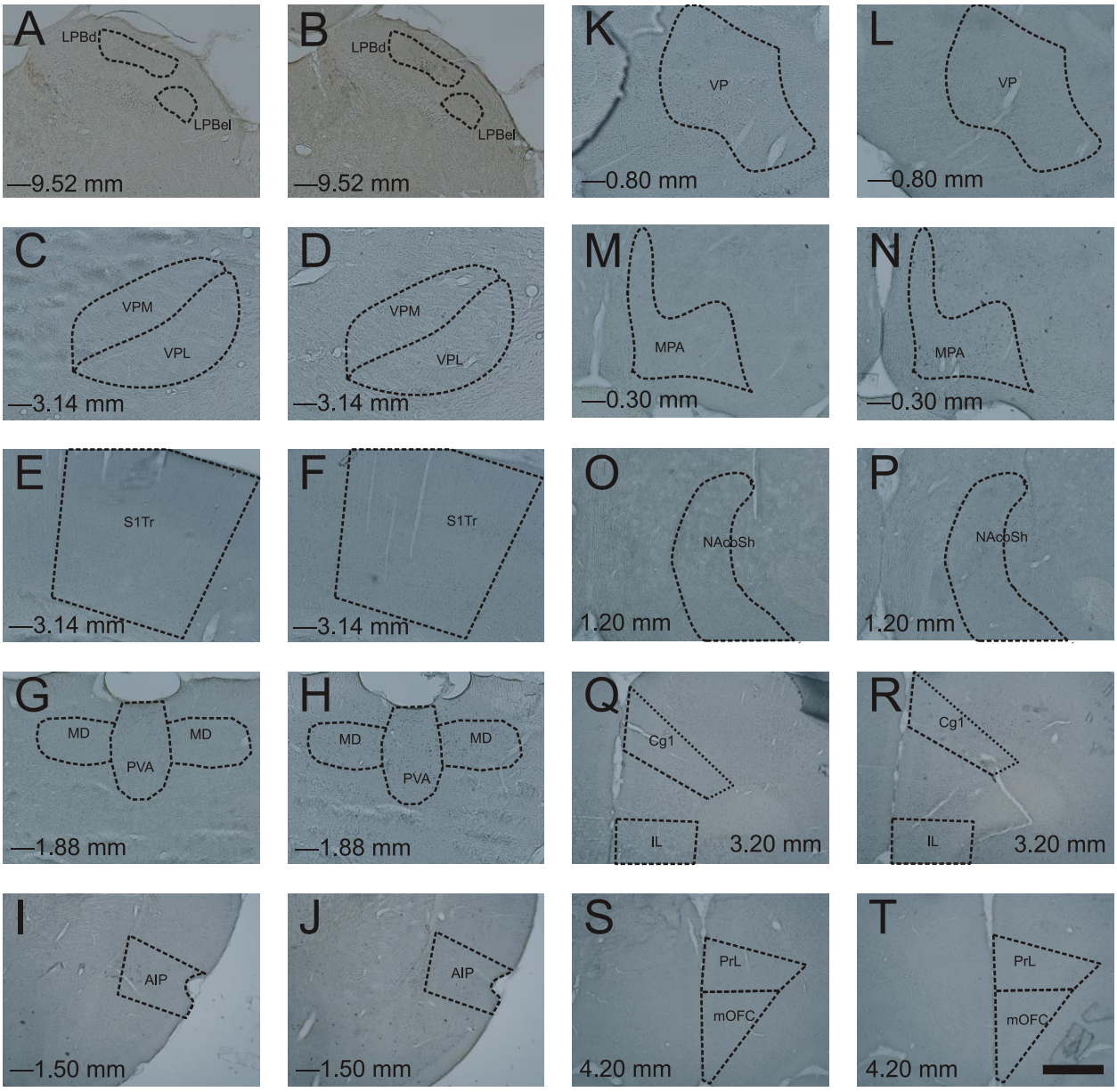

Figure 6. Low power photomicrographs illustrating c-Fos immunostaining in 18 subdivisions sampled in this study. Eleven rostrocaudal levels were sampled including, in mm from bregma: AB) −9.52 mm, BCEF) −3.14 mm, GH) −1.88 mm, IJ) −1.50 mm, KL) −0.80 mm, MN) −0.30 mm, OP) 1.20 mm, QR) 3.20 mm, and ST) 4.20 mm (−9.34 mm and −9.70 mm are not included in this figure). The subdivisions that were sampled are illustrated with dashed lines. Grids were placed entirely inside the areas indicated. Refer to Table 3 or Figure 2 for the area counted. For abbreviations, see *Abbreviations*. All images were taken at 40x magnification (4x objective). Scale bar: 500 µm.

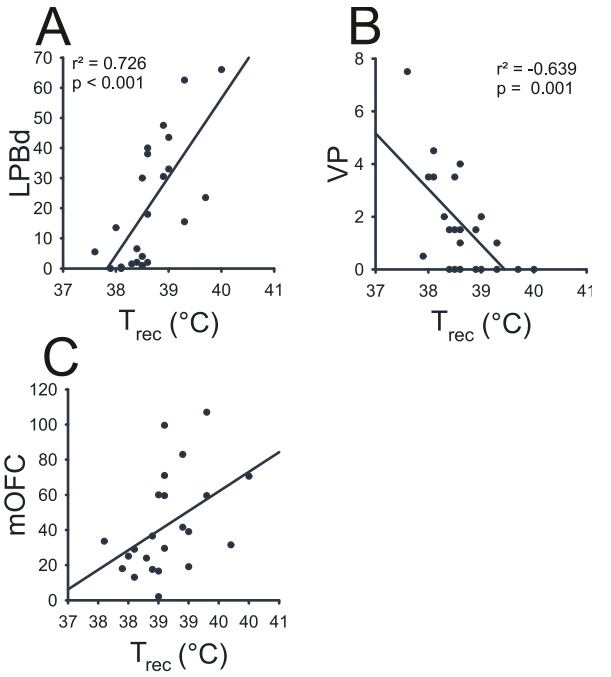

Figure 7. Scatter plots depicting the relationship between the numbers of c-Fos-ir cells counted in the A) $LPBd_{total}$, B) VP and C) mOFC and rectal temperature (T_{rec}) of individual rats. For abbreviations, see *Abbreviations*. Each dot represents a single rat. Pearson 2-tailed correlation.

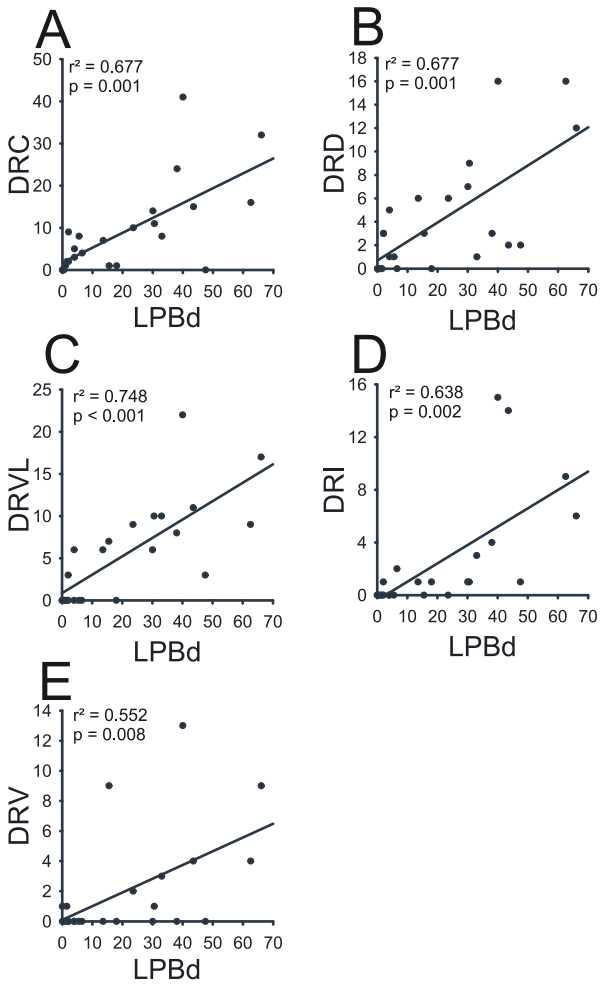

Figure 8. Scatter plots depicting the relationship between the numbers of c-Fos-ir cells counted in the $LPBd_{total}$ and correlations with DR subdivisions including A) DRC, B) DRD, C) DRVL, D) DRI, and E) DRV of individual rats. For abbreviations, see *Abbreviations*. Each dot represents a single rat. Pearson 2-tailed correlation.

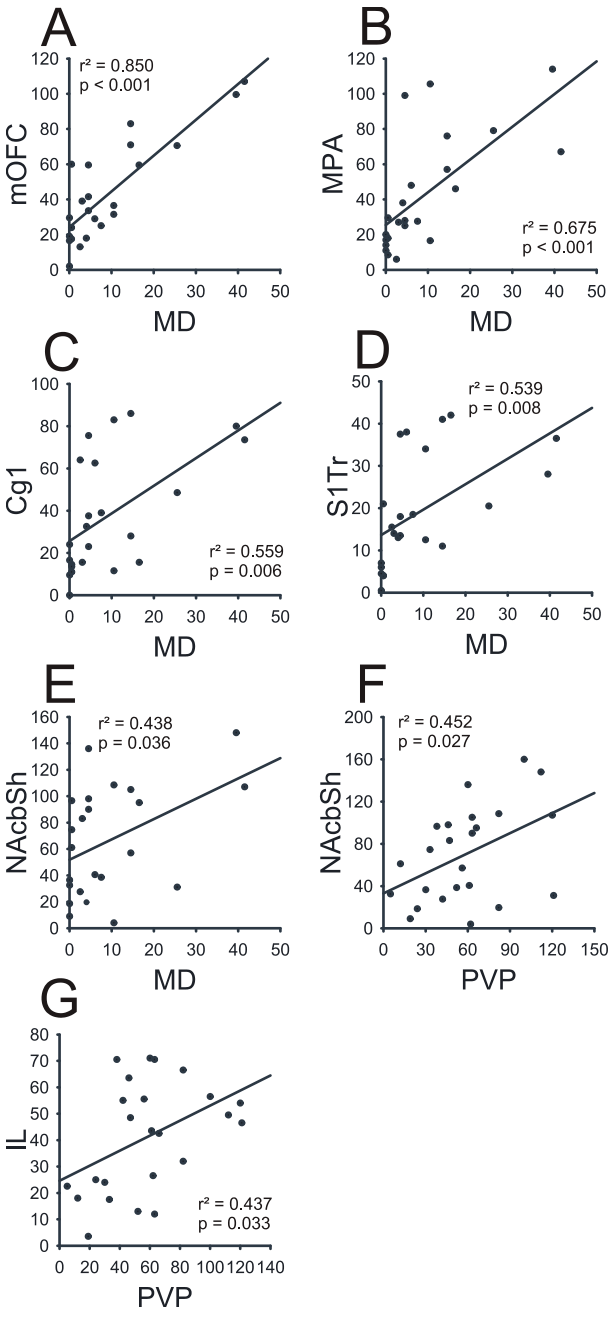

Figure 9. Scatter plots depicting the relationship between the numbers of c-Fos-ir cells counted in the MD and PVP (x-axis) and correlations with the numbers of c-Fos-ir cells counted in various thermoregulatory, discriminative, and affective subdivisions (y-axis) of individual rats. Subdivisions correlated with the MD nucleus include the A) mOFC, B) MPA, C) Cg1, D) S1Tr, and E) NAcbSh. Cortical structures correlated with the PVP nucleus include the F) NAcbSh, and G) IL. For abbreviations, see *Abbreviations*. Each dot represents a single rat. Pearson 2-tailed correlation.

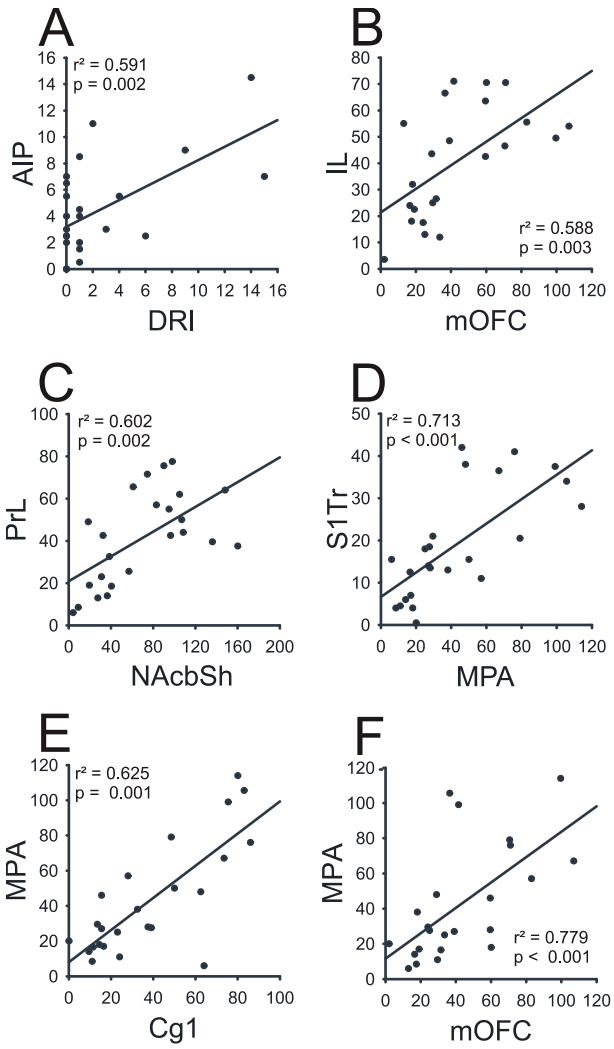

Figure 10. Scatter plots depicting the relationship between the numbers of c-Fos-ir cells counted in various subdivisions implicated in thermoregulatory, discriminative, and affective circuitry (x- and y-axis) or to T_{rec}. For abbreviations, see *Abbreviations.*

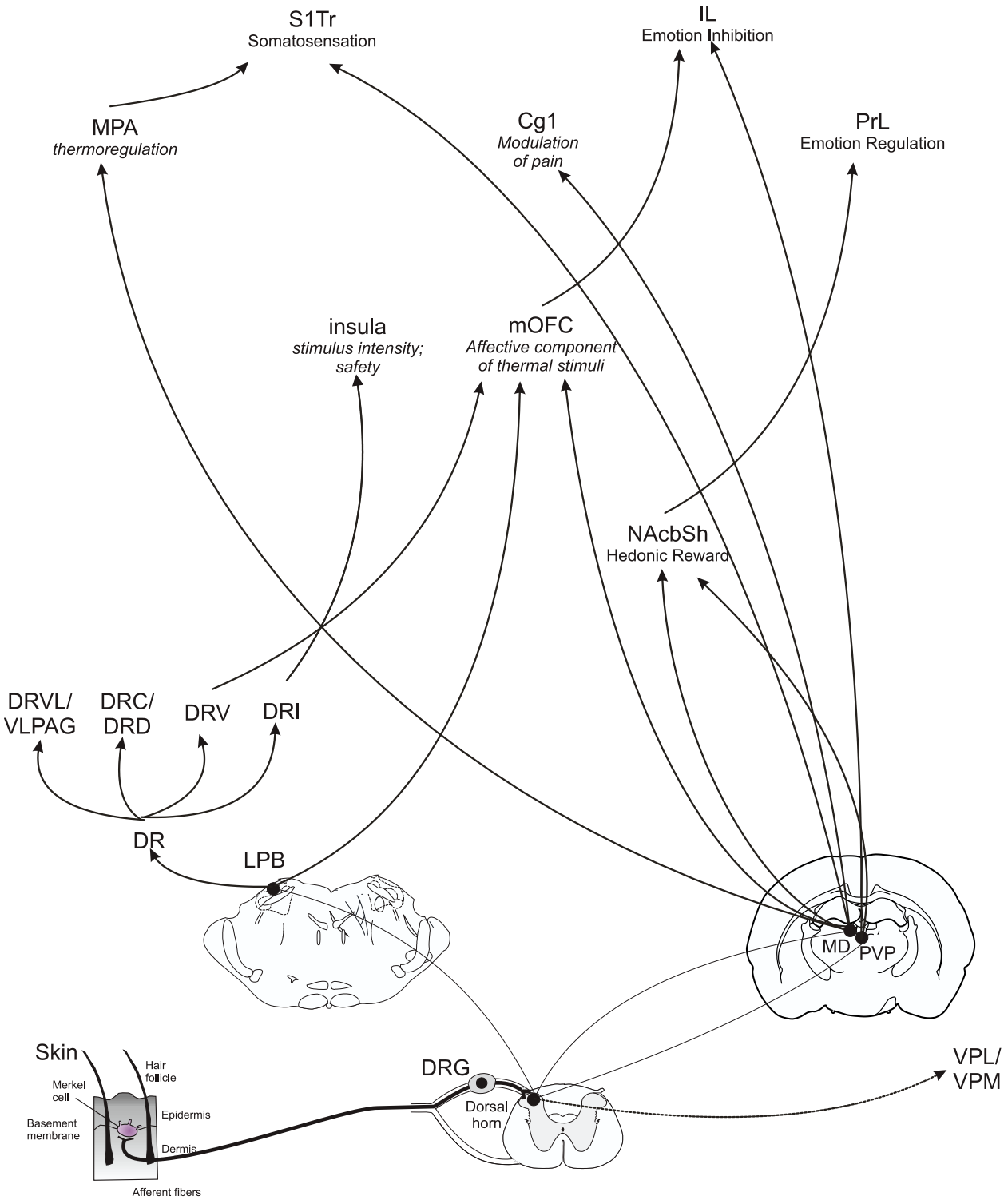

Figure 11. Hypothetical model illustrating spinoparabrachial and spinothalamic pathways and their cortical and basal forebrain targets. For correlations see Table 2 and Table 3. For abbreviations, see *Abbreviations.*